Rôle de la zone endommagée sur la convergence des galeries de stockage, modélisation numérique d'expériences dans le laboratoire souterrain de Bure

Frédéric COLLIN, Université de Liege
Robert CHARLIER, Université de Liege
Benoît PARDOEN, Université de Louvain

Journée d'études SBGIMR sur le stockage géologique de déchets nucléaires
Liège, 21 février 2019

Long-term management of radioactive wastes

Intermediate
(long-lived)
&
high activity
wastes

Deep geological disposal

Repository in deep geological media with good confining properties

(Low permeability $K<10^{-12}$ m/s)

Underground structures

= network of galleries

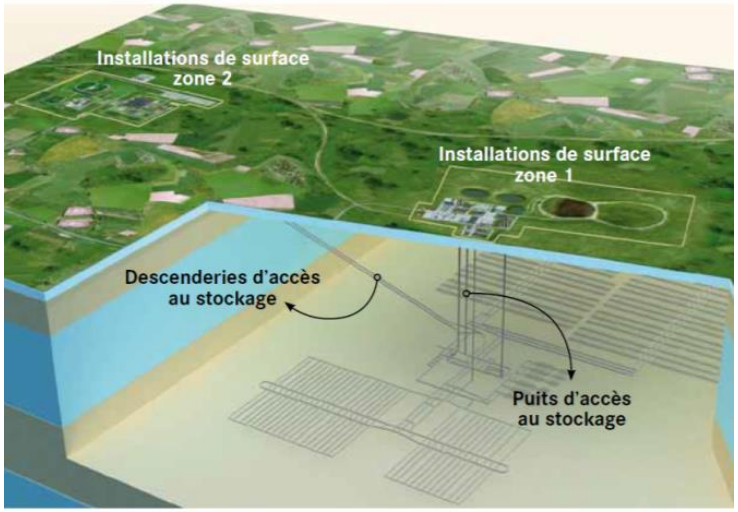

Disposal facility of Cigéo project in France
(Labalette et al., 2013)

Callovo-Oxfordian claystone (COx)

Sedimentary clay rock (France).

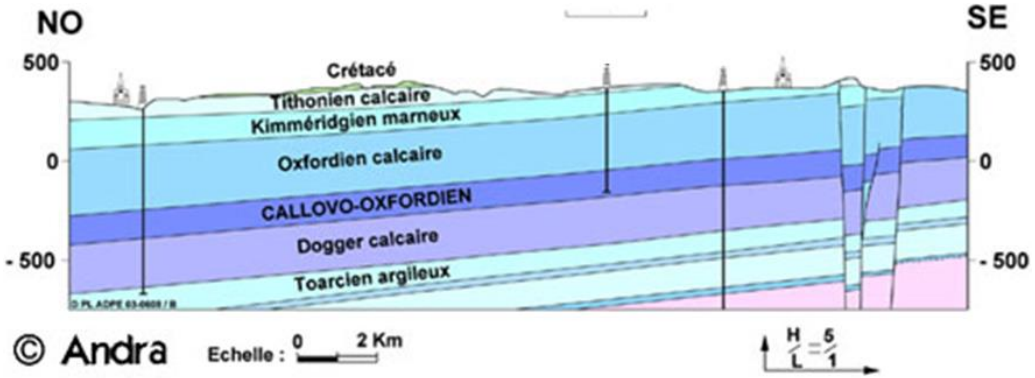

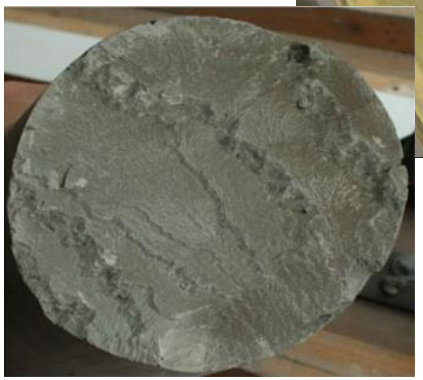

Borehole core samples
(Andra, 2005)

- Underground research laboratory

Feasibility of a safe repository

France (Meuse / Haute-Marne, Bure)

(Armand et al., 2014)

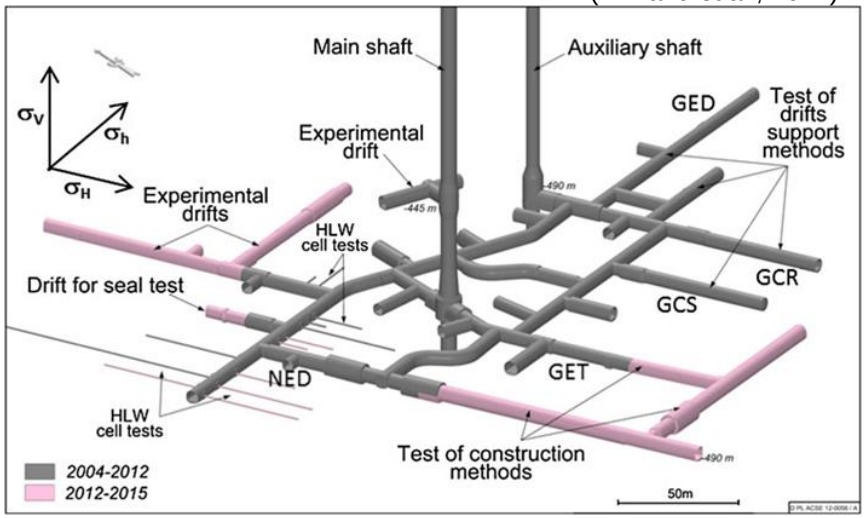

Repository phases

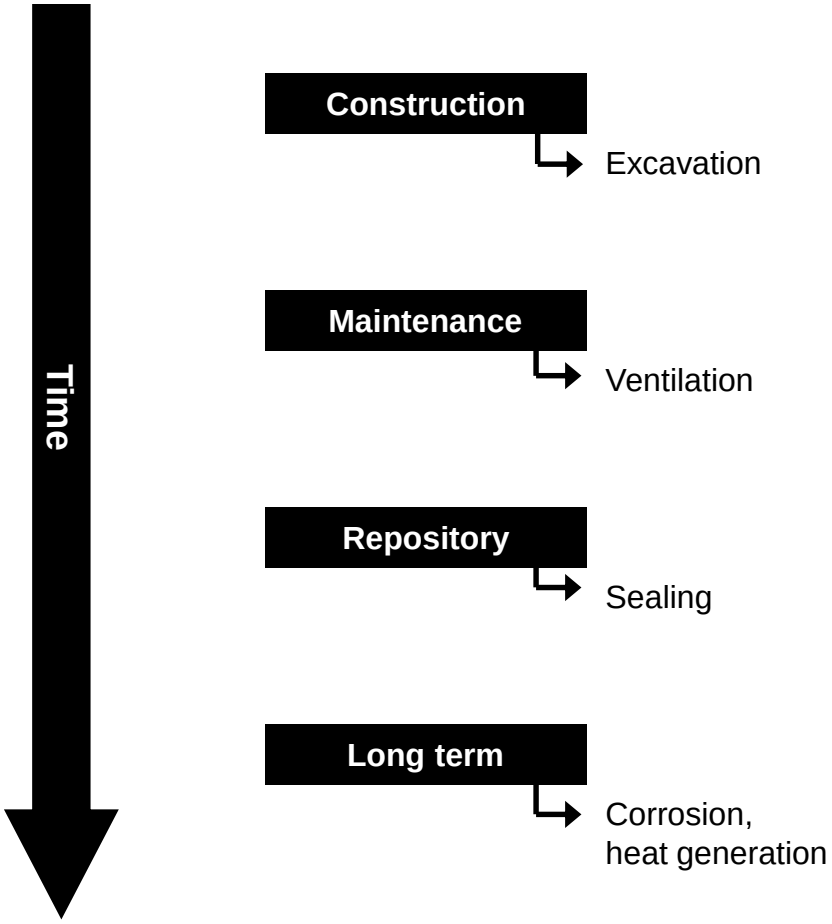

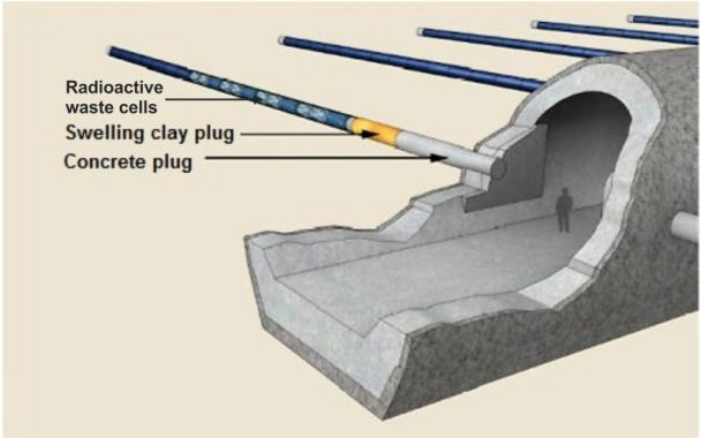

Type C wastes (Andra, 2005)

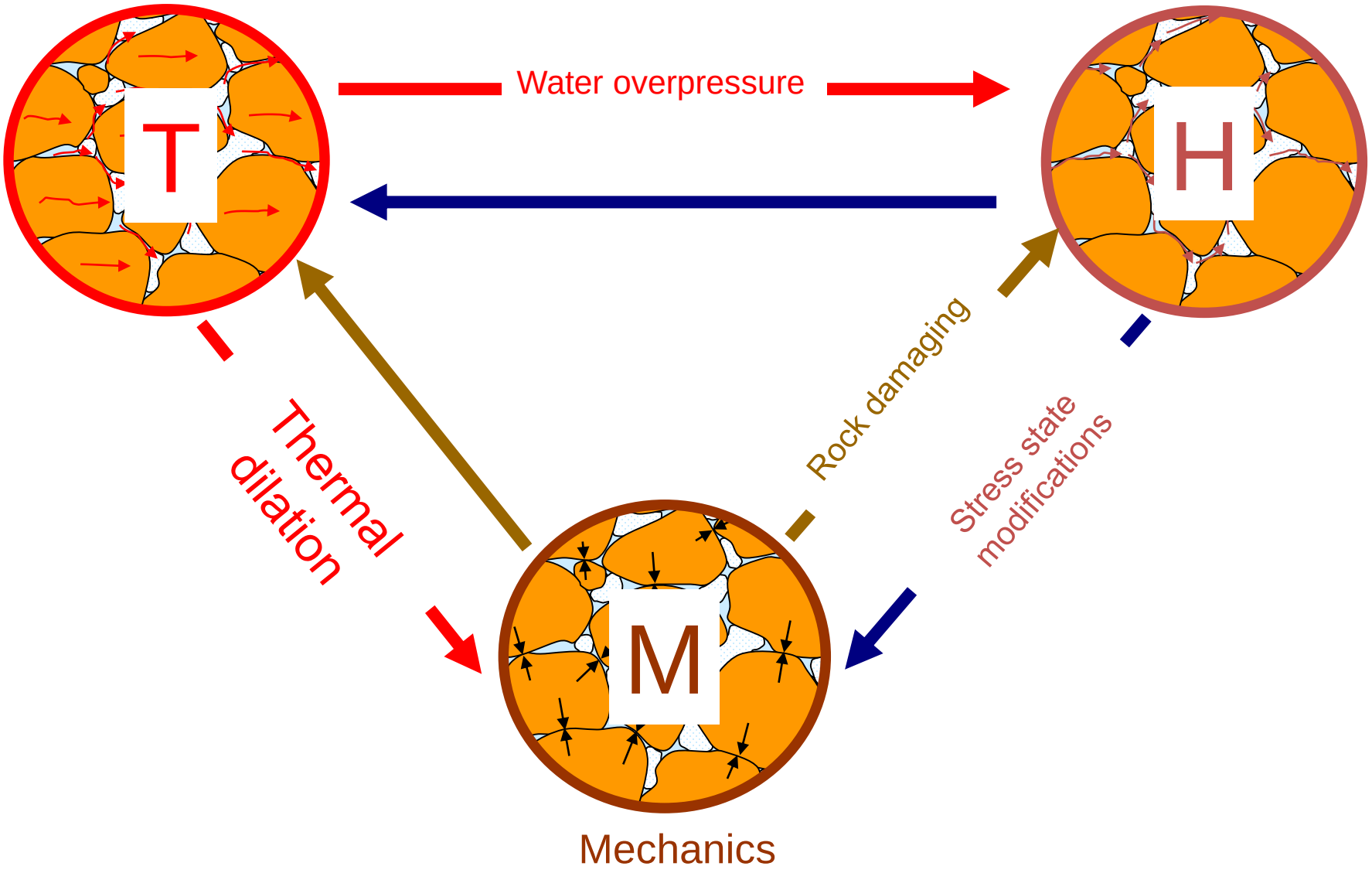
Heat transfer
Water and gas flow
T
H
M
Water overpressure
Thermal dilation
Rock damaging
Stress state modifications
Mechanics

Repository phases

Time

Construction → Excavation

Maintenance → Ventilation

Repository → Sealing

Long term → Corrosion, heat generation

Type C wastes (Andra, 2005)

Excavation Damaged Zone (EDZ)

Construction
Mechanical fracturing

- Excavation
- ↓
- Stress redistribution
- ↓
- Damage / Fracturing
- ↓
- **Coupled processes**
  HM property modifications
- ↓
- Safety function alteration

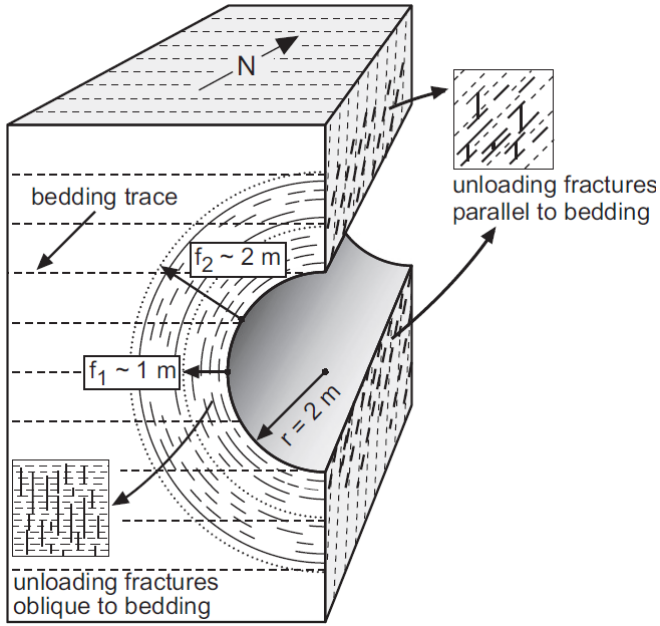

Fracturing & permeability increase
(several orders of magnitude)

Opalinus clay in Switzerland
(Bossart et al., 2002)

Maintenance
Water transfer

- Galleries ventilation
- ↓
- Air-rock interaction
- ↓
- Drainage / desaturation
- ↓
- Modification of the
  water transfer

1. Context

- Fracturing

Anisotropies: - stress : $\sigma_H > \sigma_h \sim \sigma_v$

- material : HM cross-anisotropy.

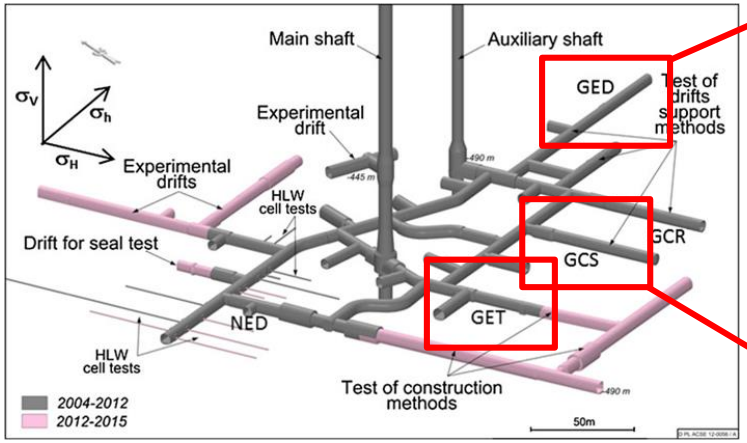

Galery // to σ_h

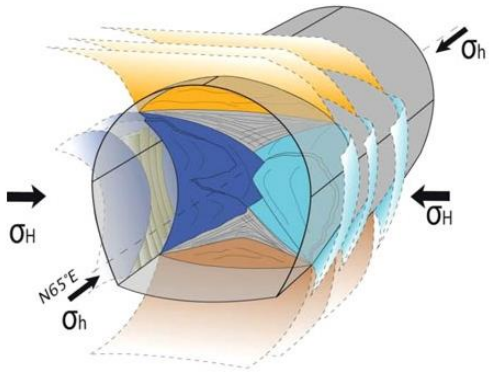

(Armand et al., 2014)

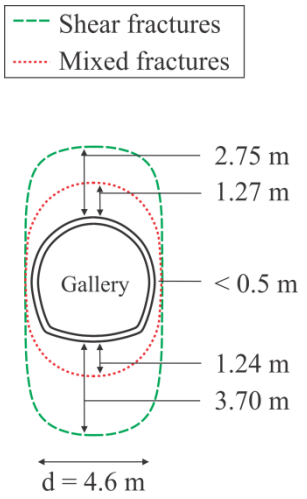

Galery // to σ_H

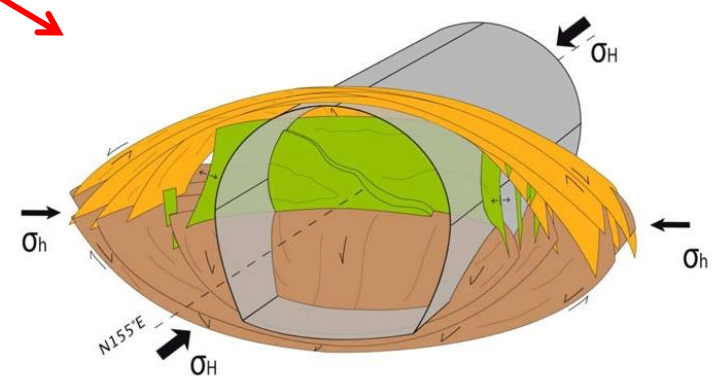

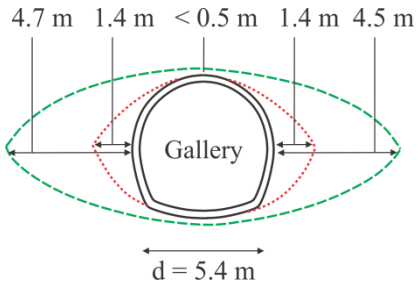

Issues: Prediction of the fracturing.
Effect of anisotropies ?
Permeability evolution & relation to fractures ?

Outline

1. Context
2. **Fracture modelling with shear bands**
3. Influence of mechanical anisotropy
4. Permeability evolution and water transfer
5. Conclusions and perspectives

2.1. Material rupture

- Compression test on small sample

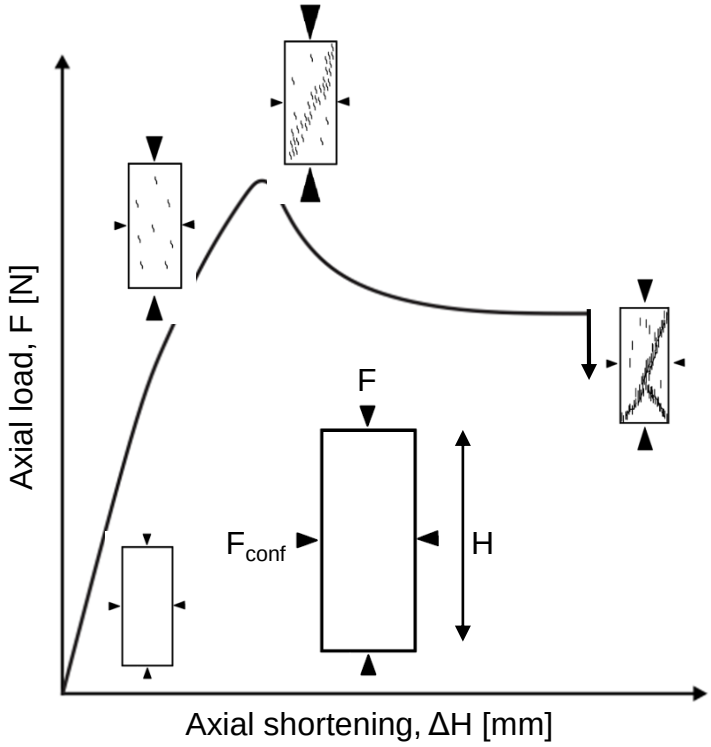

- Mechanisms of rock mass failure around gallery

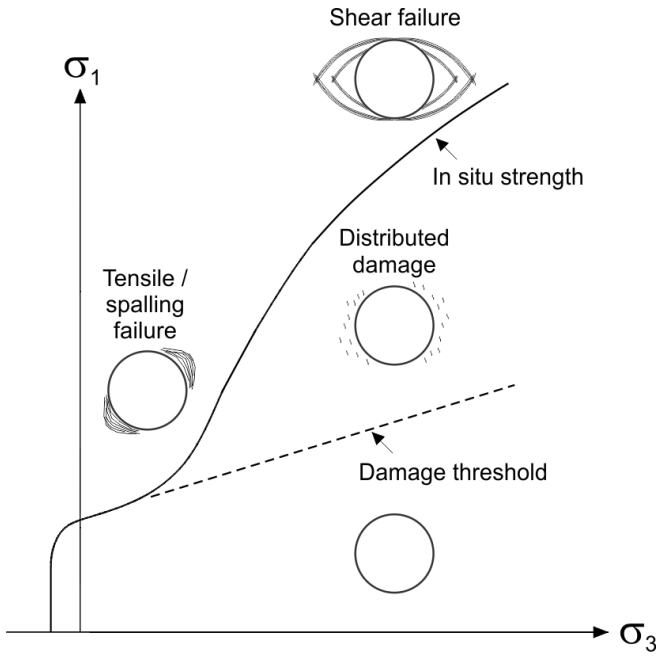

(after Diederichs, 2003)

- Fracture modelling

Shear bands are observed in many geomaterials.

COx : 75% of fractures in mode II (shear).

→ Shear strain localisation (continuous approach)

2.2. Constitutive models for COx

- Mechanical law - 1st gradient model

Isotropic elasto-plastic internal friction model

Non-associated plasticity, Van Eeckelen yield surface :

$$F \equiv II_{\hat{\sigma}} - m\left(I_{\sigma'} + \frac{3\,c}{\tan\varphi_C} \right) = 0$$

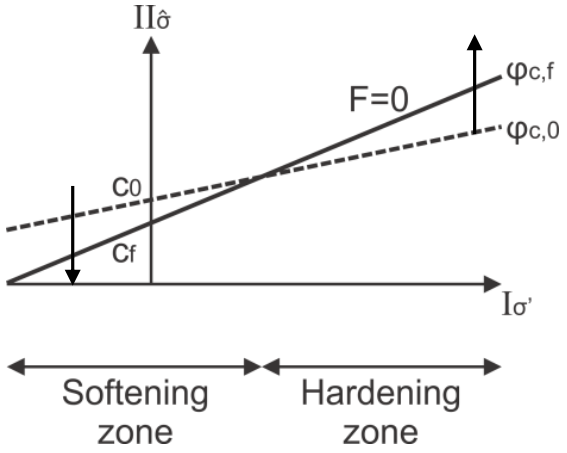

φ hardening / c softening

$$c = c_0 + \frac{\left(c_f - c_0\right)\hat{\varepsilon}^p_{eq}}{B_c + \hat{\varepsilon}^p_{eq}}$$

→ Strain localisation

- Hydraulic law

Fluid mass flow (advection, Darcy) : $$f_{w,i} = -\rho_w \frac{k_{w,ij}\, k_{r,w}}{\mu_w}\left(\frac{\partial p_w}{\partial x_j} + \rho_w\, g_j \right)$$

Water retention and permeability curves (Mualem - Van Genuchten's model)

2.3. Gallery excavation modelling

- Numerical model

HM modelling in 2D
plane strain state

Gallery radius = 2.3 m

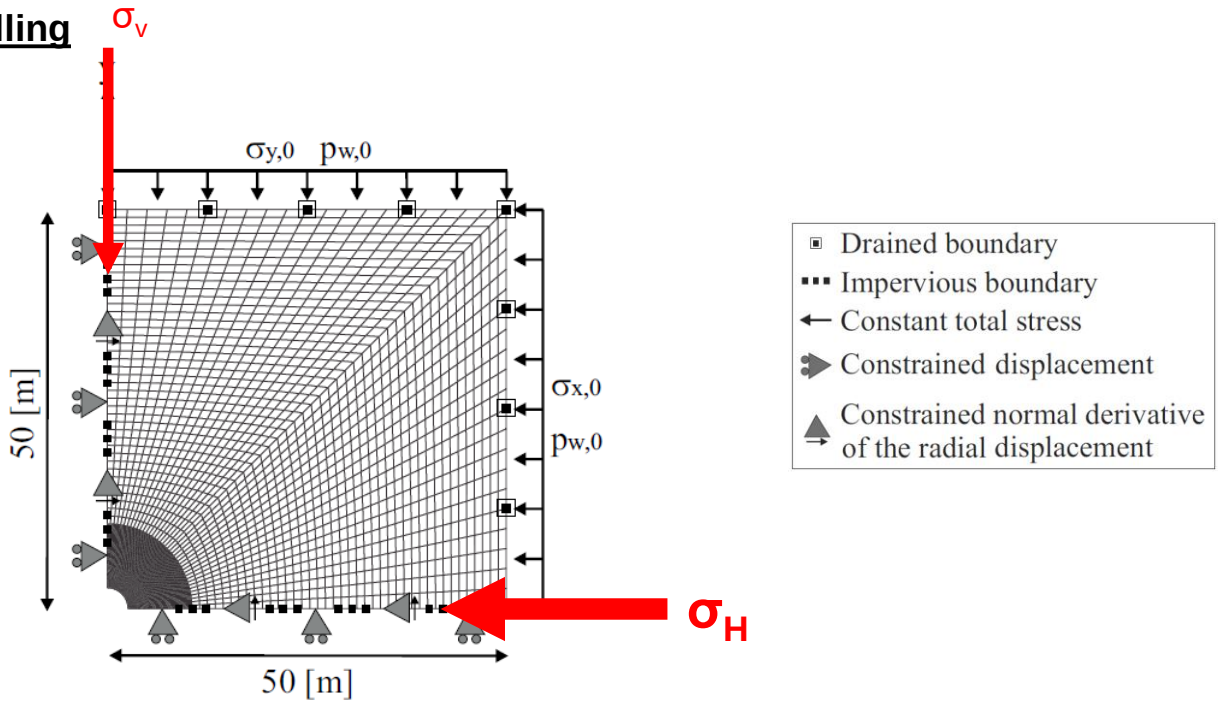

- Gallery in COx // σ_h

Effect of stress anisotropy

Anisotropic stress state

$p_{w,0}$ = 4.5 [MPa]

$\sigma_{x,0} = \sigma_H$ = 1.3 σ_v = 15.6 [MPa]

$\sigma_{y,0} = \sigma_v$ = 12 [MPa]

$\sigma_{z,0} = \sigma_h$ = 12 [MPa]

- Excavation

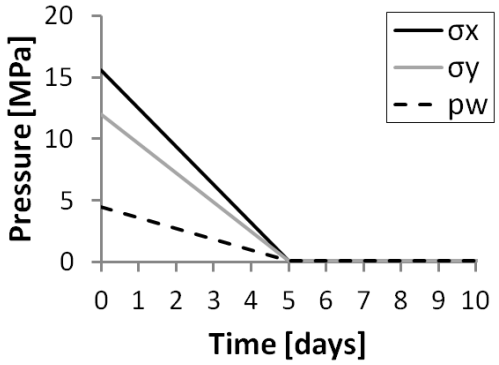

2. Fracture modelling with shear bands

- Localisation zone

Incompressible solid grains, b=1

Total deviatoric strain

Plasticity

1009 days

End of excavation

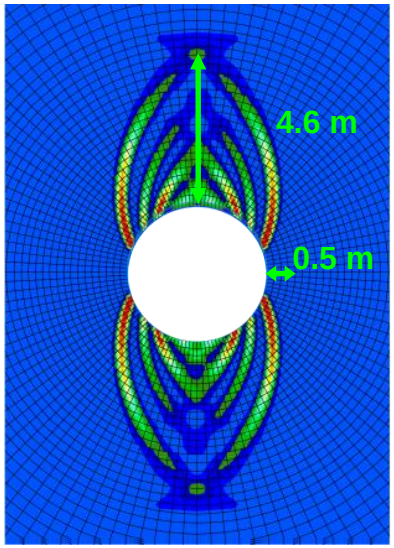

$$\hat{\varepsilon}_{eq} = \sqrt{\frac{2}{3}\hat{\varepsilon}_{ij}\hat{\varepsilon}_{ij}}$$

0 0.06

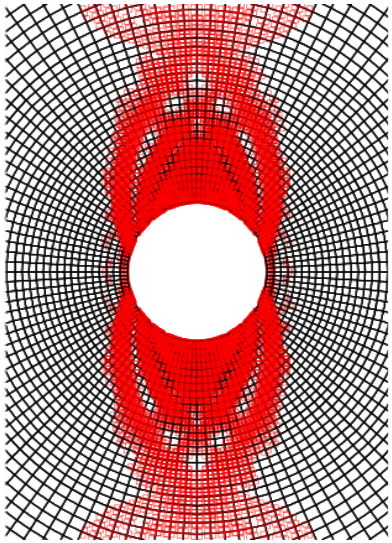

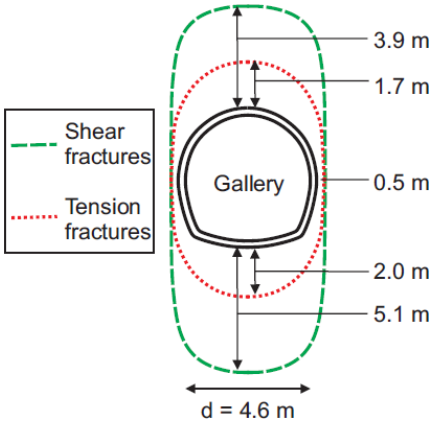

→ For an isotropic mechanical behaviour, the appearance and shape of the strain localisation are mainly due to mechanical effects linked to the anisotropic stress state.

2. Fracture modelling with shear bands

- Gallery air ventilation :

Water phases equilibrium at gallery wall (Kelvin's law)

$$RH = \frac{p_v}{p_{v,0}} = exp\left(\frac{-p_c M_v}{RT \rho_w}\right)$$

Compressibility of the solid grains: b=0.6

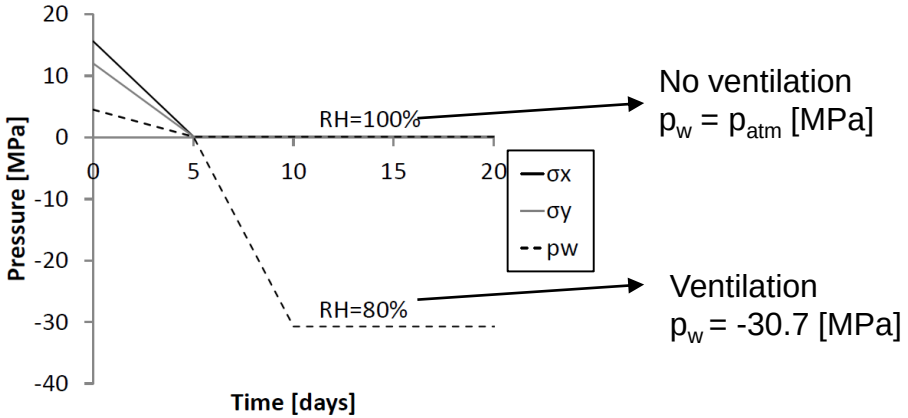

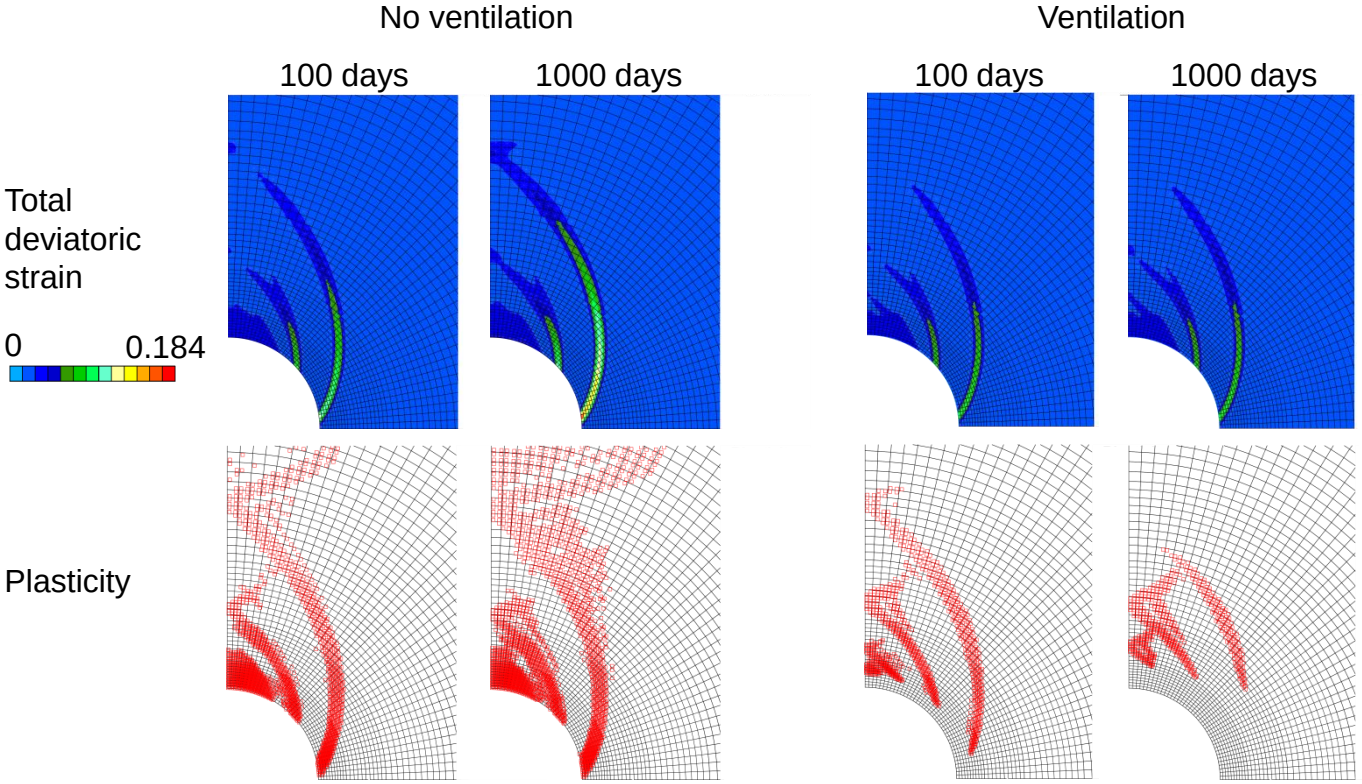

$$\sigma_{ij} = \sigma'_{ij} + b\, S_{r,w}\, p_w\, \delta_{ij}$$

→ suction ↑

→ σ' ↑

→ Elastic unloading

→ Inhibition of localisation

→ Restrain ε

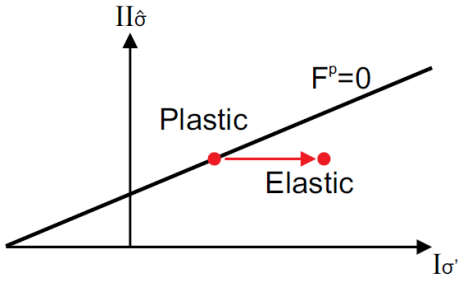

- Convergence:

Important during the excavation
Anisotropic convergence
Influence of the ventilation
Experimental results (GED - Andra's URL)
No strain localisation

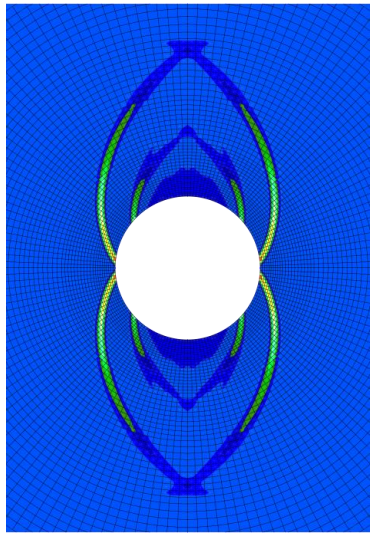

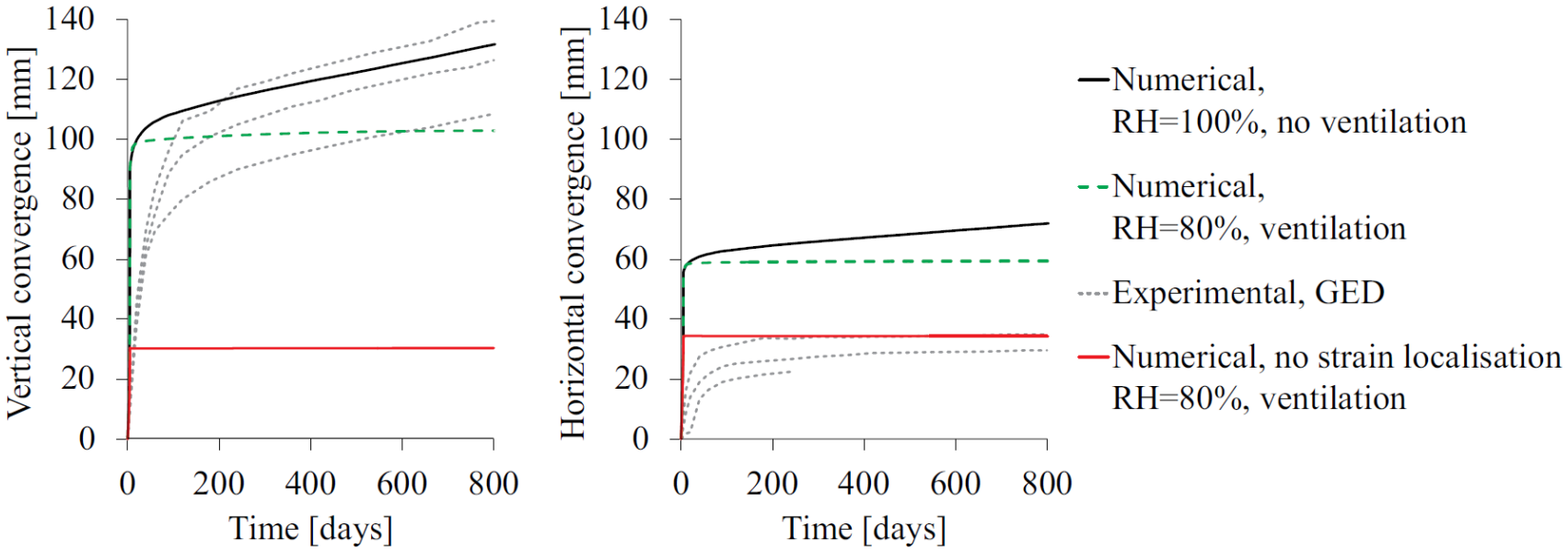

2.5. Conclusions and outlooks

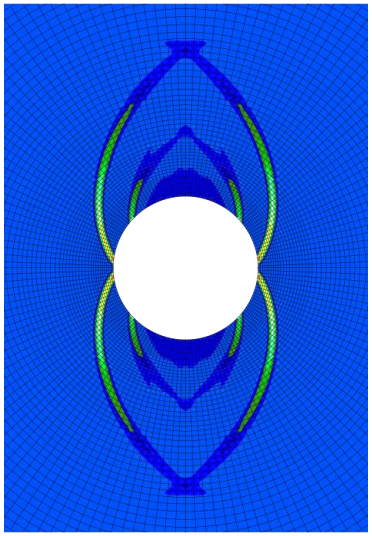

- Conclusions

✓ Reproduction of EDZ with shear bands.

✓ Shape and extent of EDZ **governed by anisotropic stress state.**

- Next steps …

X Mechanical rock behaviour.

→ Material anisotropy, gallery // σ_H .

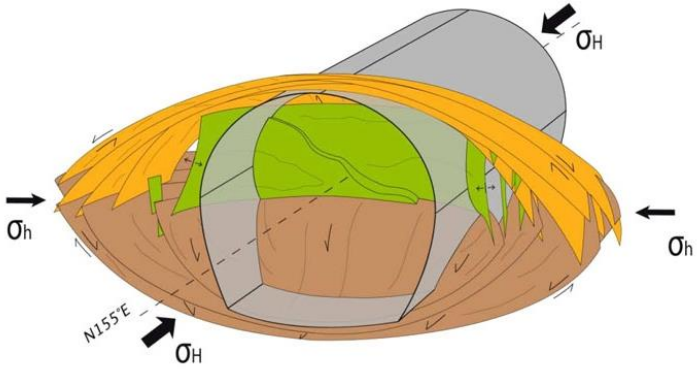

X HM coupling in EDZ.

→ Influence of fracturing on hydraulic properties.

X Gallery air ventilation and water transfer (drainage / desaturation).

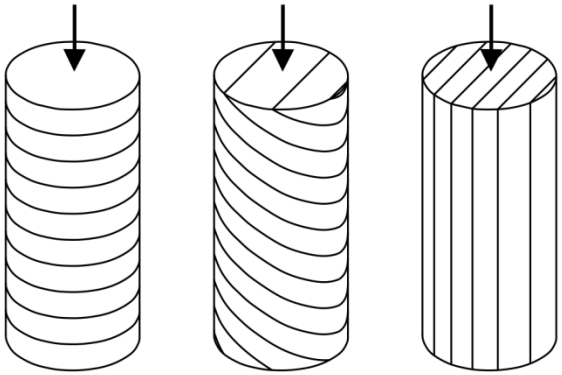

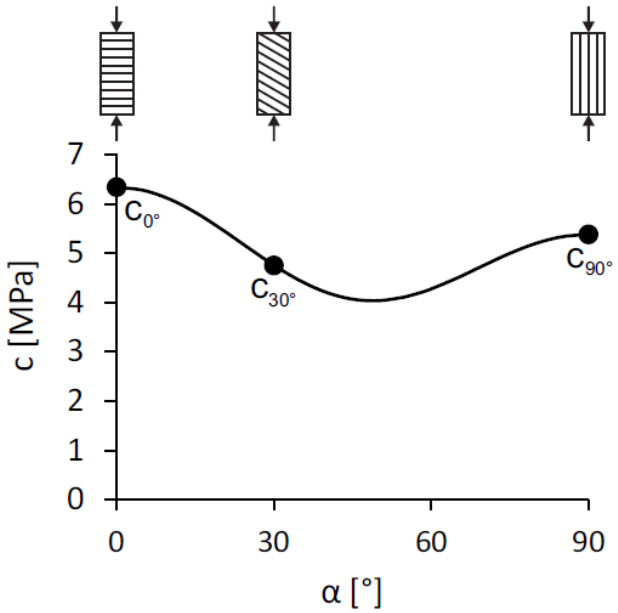

- Linear elasticity :

Cross-anisotropic (5 param.) + Biot's coefficients

$$E_{//}, E_{\perp}, \nu_{////}, \nu_{//\perp}, G_{//\perp} \qquad b_{//}, b_{\perp}$$

- Plasticity :

Cohesion anisotropy with fabric tensor

$$c_0 = a_{ij}\, l_i\, l_j \qquad l_i = \sqrt{\frac{\sigma'^2_{i1} + \sigma'^2_{i2} + \sigma'^2_{i3}}{\sigma'_{ij}\sigma'_{ij}}}$$

Cross-anisotropy

$$c_0 = \bar{c}\left(1 + A_{////}(1 - 3l_2^2) + b_1 A_{////}^2 (1 - 3l_2^2)^2 + \ldots\right)$$

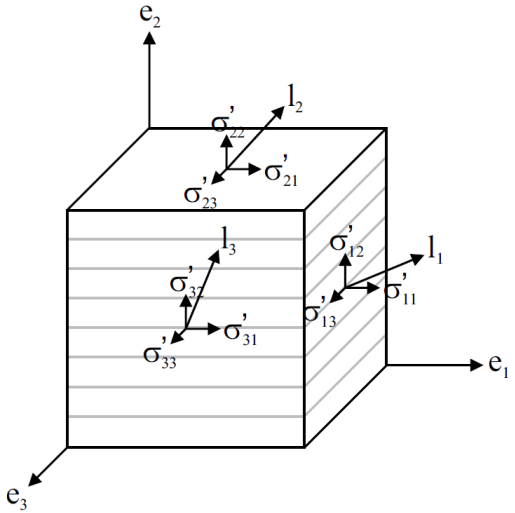

3.3. Gallery excavation modelling for anisotropic initial stress state

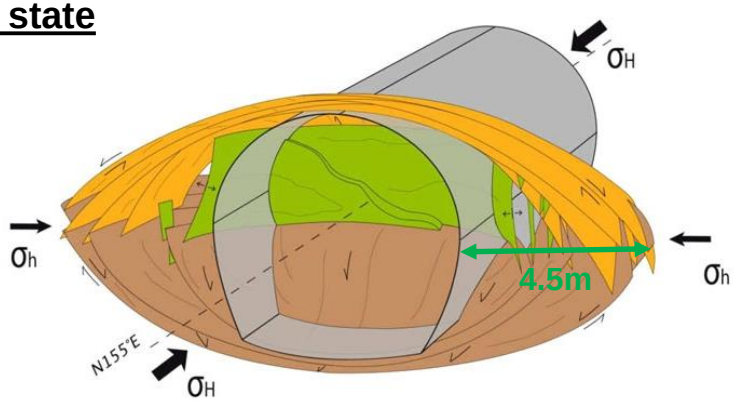

- Stress state

Major stress in the axial direction
Gallery // to σ_H

$\sigma_{x,0} = \sigma_h = 12.40$ MPa
$\sigma_{y,0} = \sigma_v = 12.70$ MPa
$\sigma_{z,0} = \sigma_H = 1.3 \times \sigma_h = 16.12$ MPa

- Shear banding

Total deviatoric strain

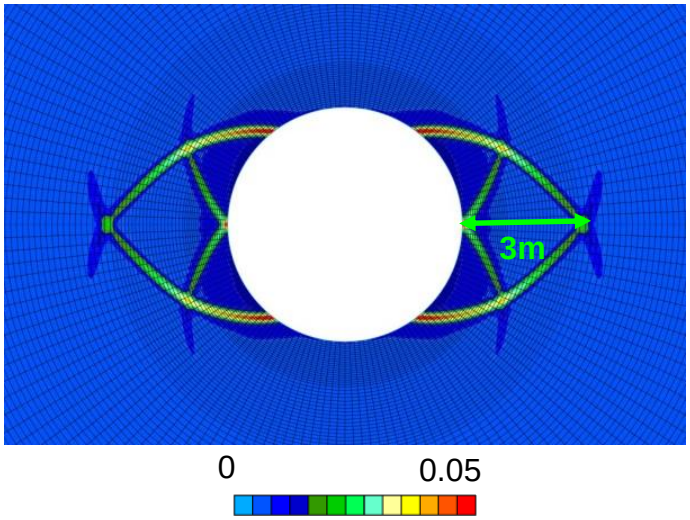

→ **Shape modification due to σ_H**

- Convergence

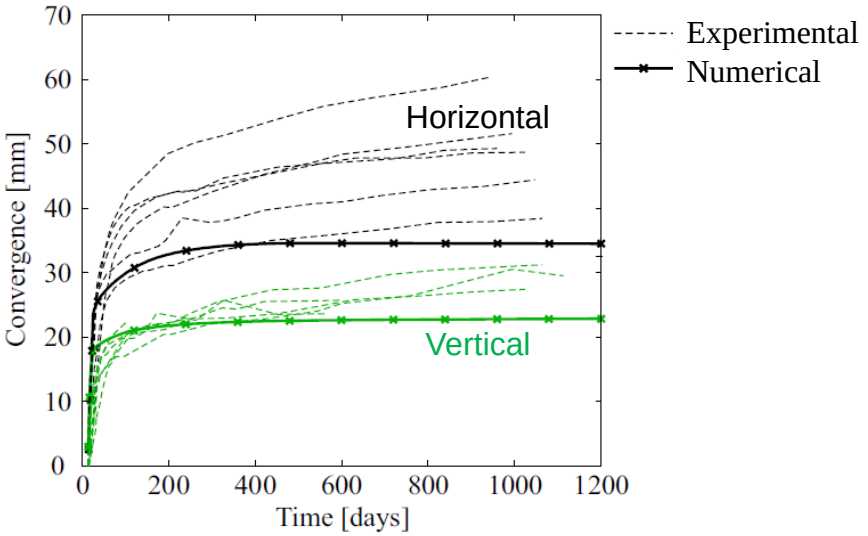

→ **Long-term deformation** → **Creep deformation**

3. Influence of mechanical anisotropy

- Creep deformation

Permanent strain

In the long term

Under constant stress
below the yield strength

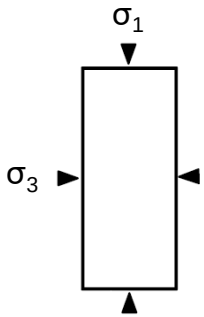

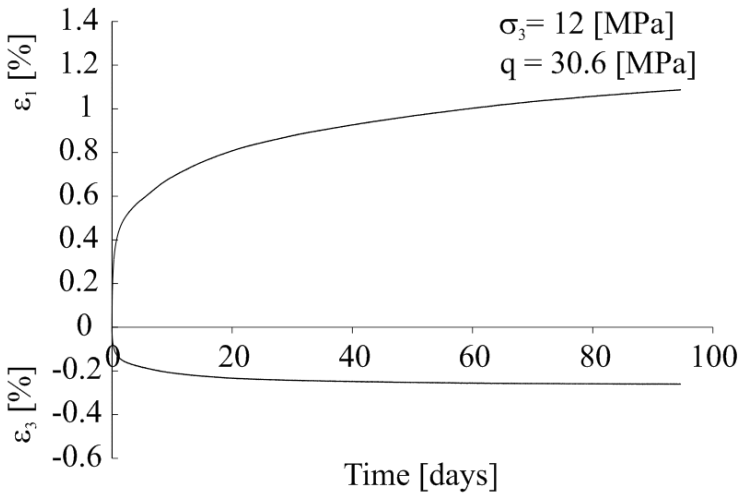

- Viscosity

Time-dependent plastic strain
(Jia et al., 2008; Zhou et al. 2008)

$$\dot{\varepsilon}_{ij} = \dot{\varepsilon}^{e}_{ij} + \dot{\varepsilon}^{p}_{ij} + \dot{\varepsilon}^{vp}_{ij}$$

$$F^{vp} \equiv \sqrt{3}\, II_{\hat{\sigma}} - \alpha^{vp} g(\beta)\, R_c \sqrt{A^{vp}\left(C^{vp} + \frac{I_{\sigma'}}{3R_c}\right)} = 0$$

- Convergence

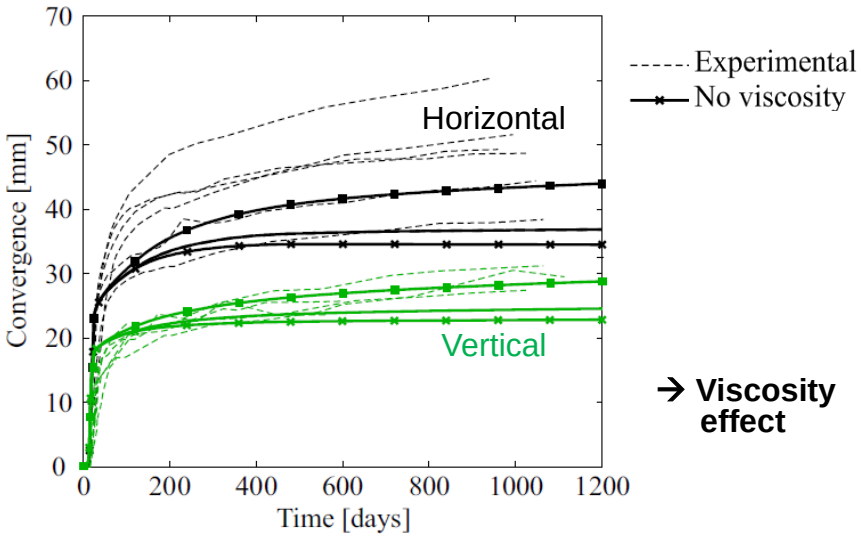

→ **Viscosity effect**

3.4. Conclusions and outlooks

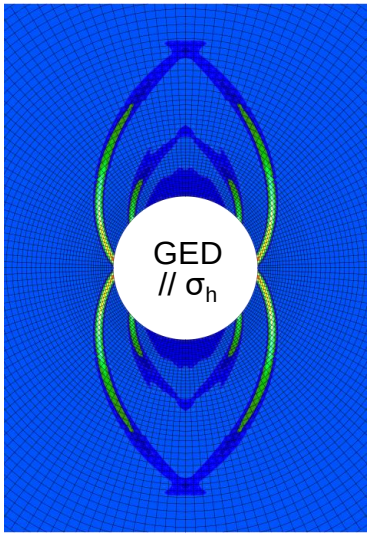

- Conclusions

✓ Reproduction of EDZ in both directions.

✓ Shape and extent of EDZ governed by**:**

- anisotropic stress state.

- anisotropic mechanical behaviour.

✓ Long-term convergence with viscosity.

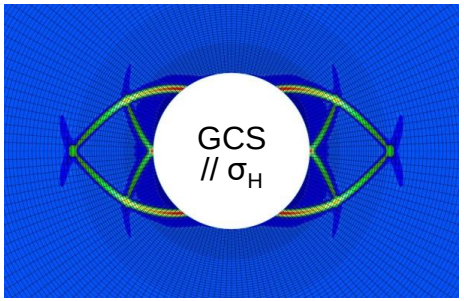

- Next steps …

X HM coupling in EDZ.

→ Influence of fracturing on hydraulic properties.

X Gallery air ventilation and water transfer.

4.1. Large-scale experiment of gallery ventilation (SDZ)

Characterise the effect of gallery ventilation
on the hydraulic transfer around it.

→ drainage / desaturation
→ exchange at gallery wall

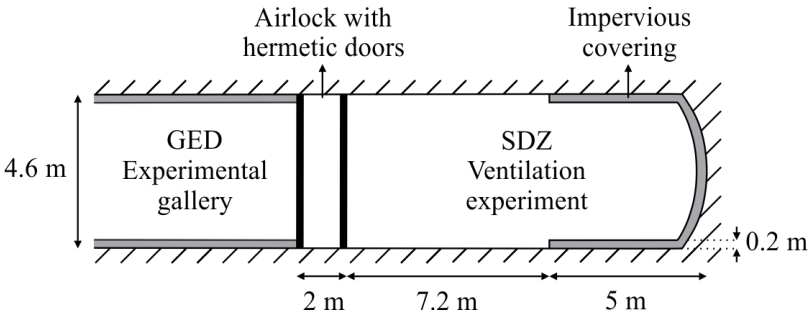

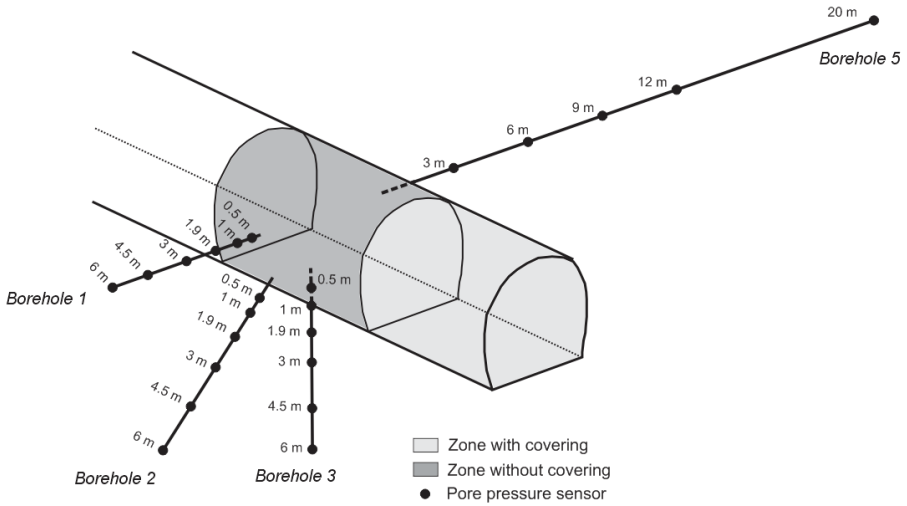

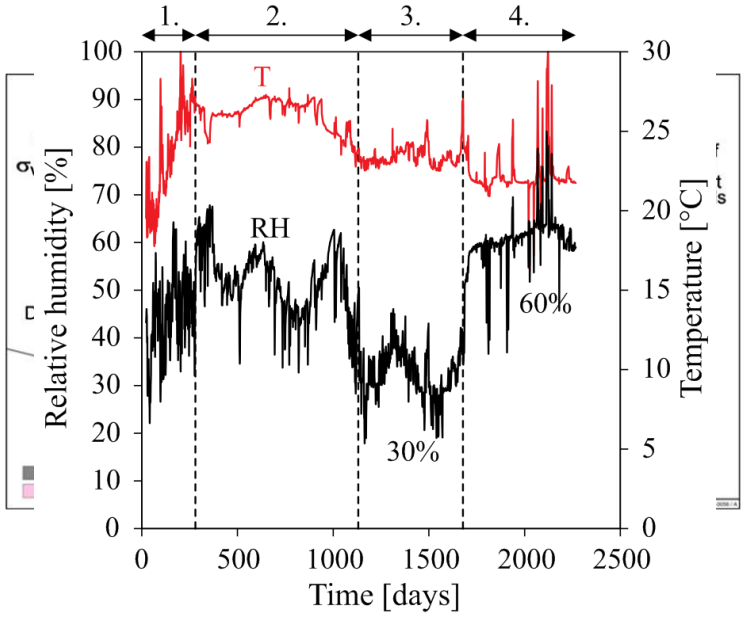

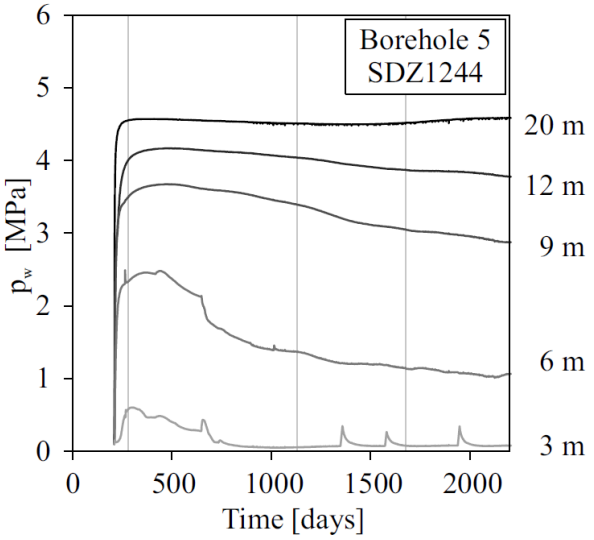

4.2. Permeability variation in fractured zone

HM coupling in the EDZ.

4.2.1. Saturated permeability in boreholes

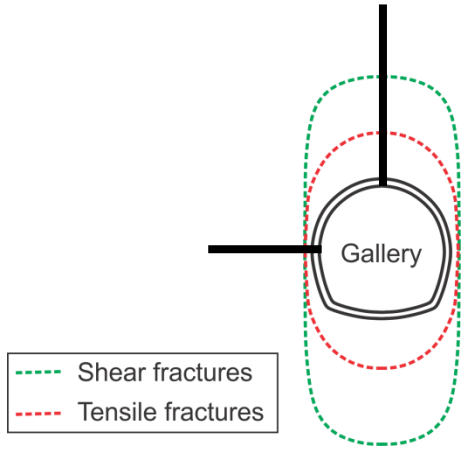

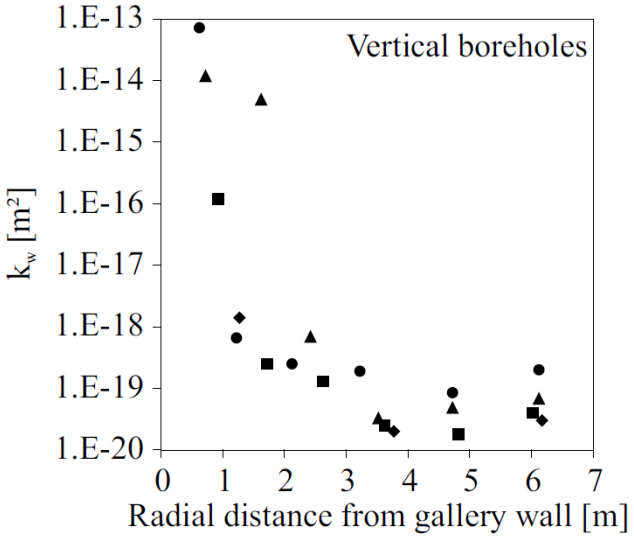

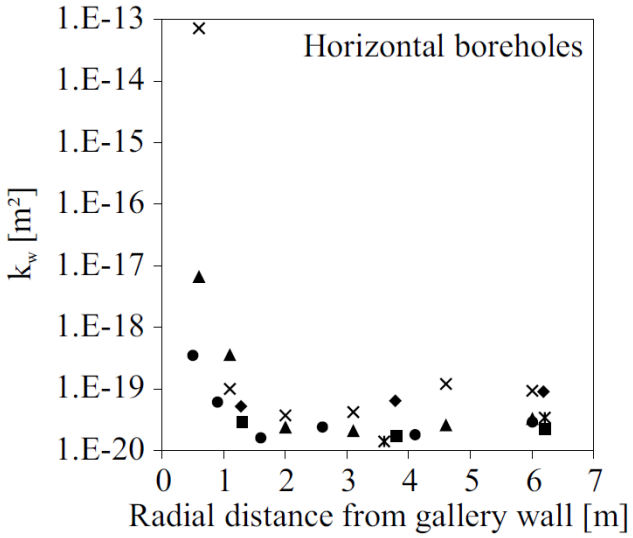

Fracture and rock matrix permeabilities

→ Capture k_w evolution

→ Relation to fractures

4.2.2. Evolution of intrinsic water permeability

Various approaches: deformation, damage, cracks…

- Relation to deformation

Volumetric effects = increase of porous space
(Kozeny-Carman)

$$k_w = k_{w,0} \frac{(1-\phi_0)^{\xi_1}}{\phi_0^{\xi_2}} \frac{\phi^{\xi_2}}{(1-\phi)^{\xi_1}} \qquad \varepsilon_v = \frac{\varepsilon_{ii}}{3}$$

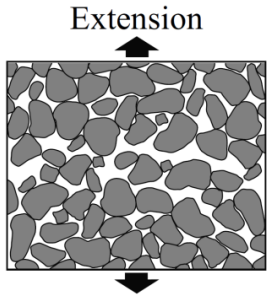

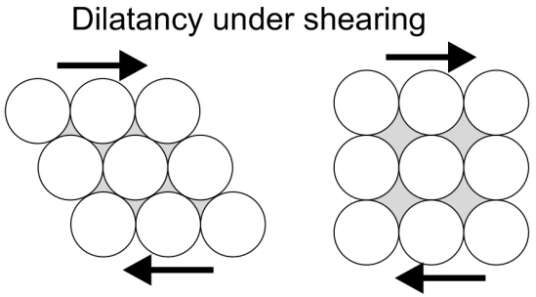

- Fracture permeability

Cubic law for parallel-plate approach
(Witherspoon 1980; Snow 1969, Olivella and Alonso 2008)

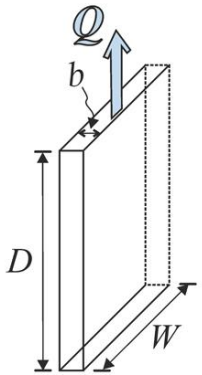

$$k_w^{cr} = \frac{b^2}{12}$$

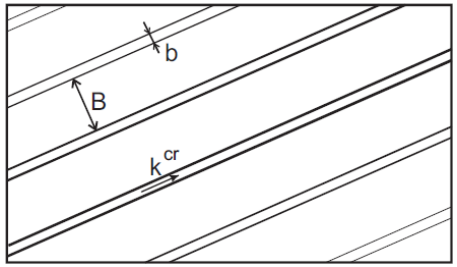

$$k_w = \frac{b^3}{12B}$$

$$b = b_0 + B\left\langle \varepsilon^n - \varepsilon_0^n \right\rangle$$

$$k_w = k_{w,0}\left(1 + A\left\langle \varepsilon^n - \varepsilon_0^n \right\rangle\right)^3$$

Localised deformation
Fracture initiation

- Empirical law

Related to strain localisation effect
Permeability variation threshold

$$k_{w,ij} = k_{w,ij,0}\left(1 + \beta_{per}\left\langle YI - YI^{thr}\right\rangle \hat{\varepsilon}_{eq}^{\ 3}\right) \qquad YI = \frac{II_{\hat{\sigma}}}{II_{\hat{\sigma}}^{p}}$$

4.4. Modelling of excavation and SDZ experiment

4.4.1. HM coupling in EDZ

- Gallery excavation

SDZ → GED gallery // σ_h

Anisotropic $\sigma_{ij,0}$ and material

→ Localisation zone dominated by stress anisotropy

Plasticity

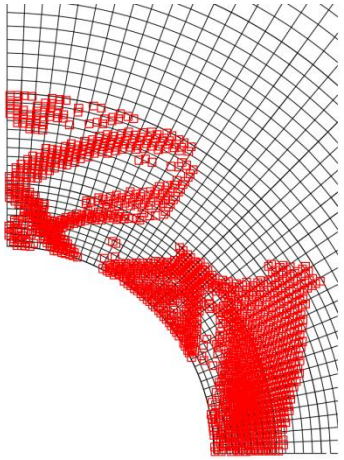

Total deviatoric strain

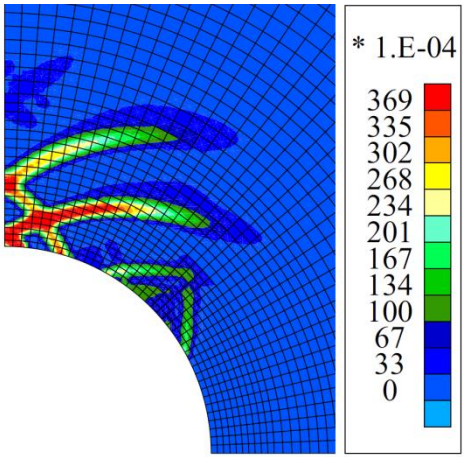

$k_{w,,ij}$ / $k_{w,ij,0}$ [-]

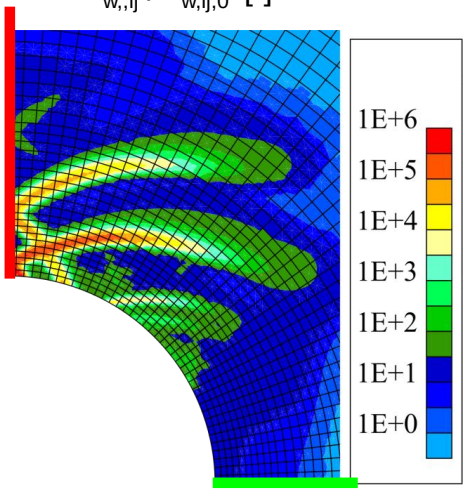

- Intrinsic permeability evolution

$$\frac{k_{w,ij}}{k_{w,ij,0}} = \left(1 + \beta \left\langle YI - YI^{thr} \right\rangle \hat{\varepsilon}_{eq}^{\,3}\right)$$

$$YI^{thr} = 0.95$$

Cross-sections

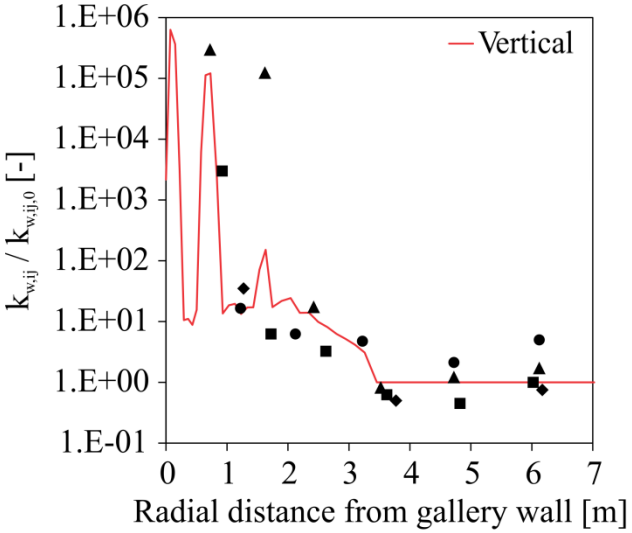

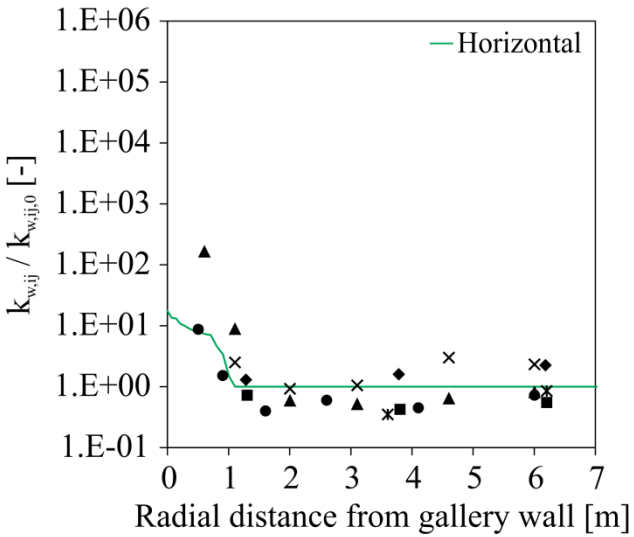

Plastic strain and a part of the elastic one → EDZ extension + k_w increase

4. Permeability evolution and water transfer

- Drainage / p_w reproduction

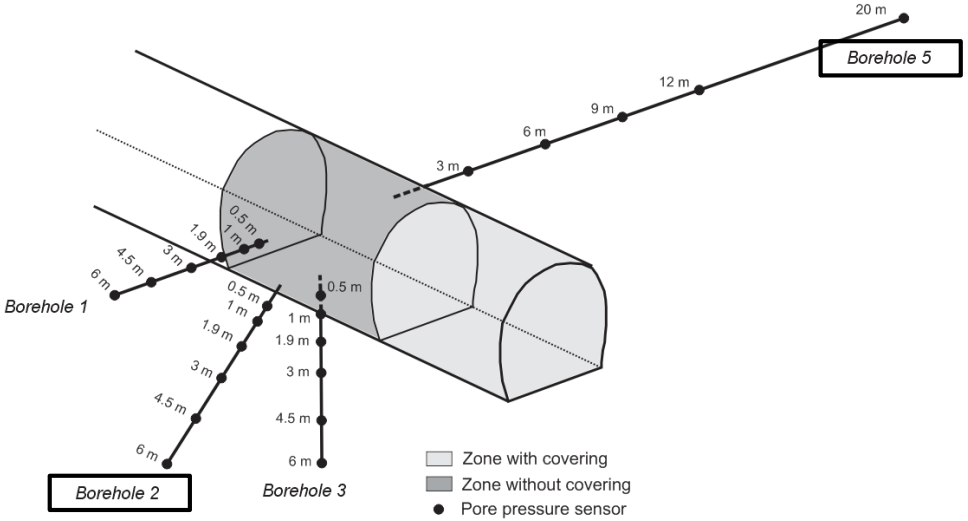

Oblique 45°

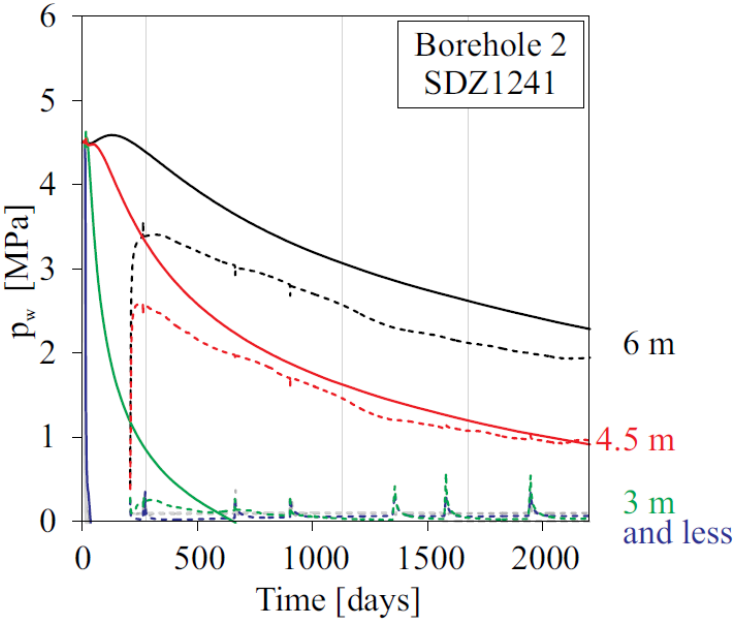

Horizontal

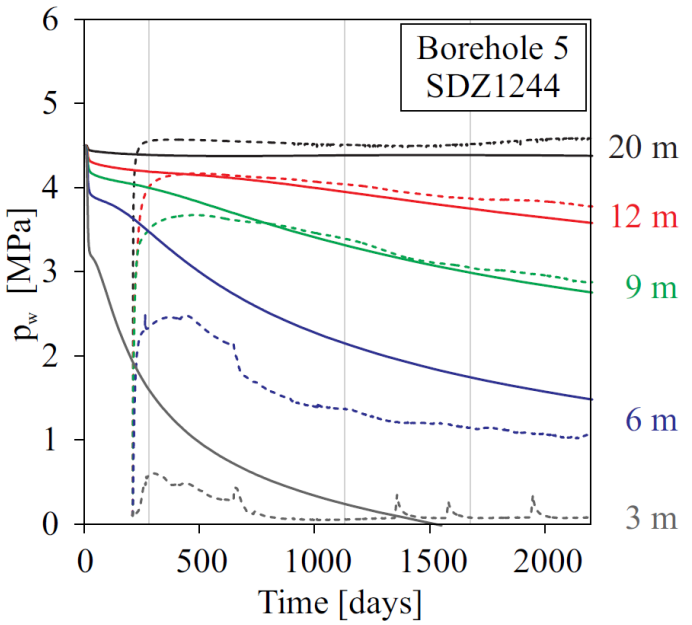

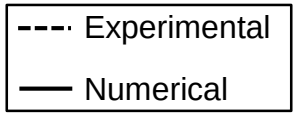

$\alpha_v = 10^{-3}$ m/s

4. Permeability evolution and water transfer

- Desaturation EDZ / w reproduction

Horizontal boreholes

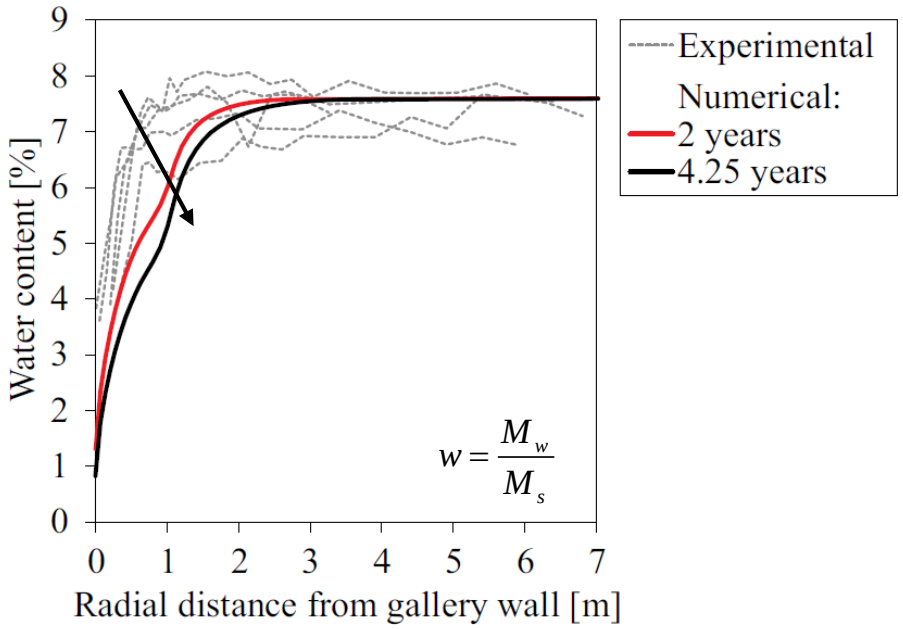

At gallery wall

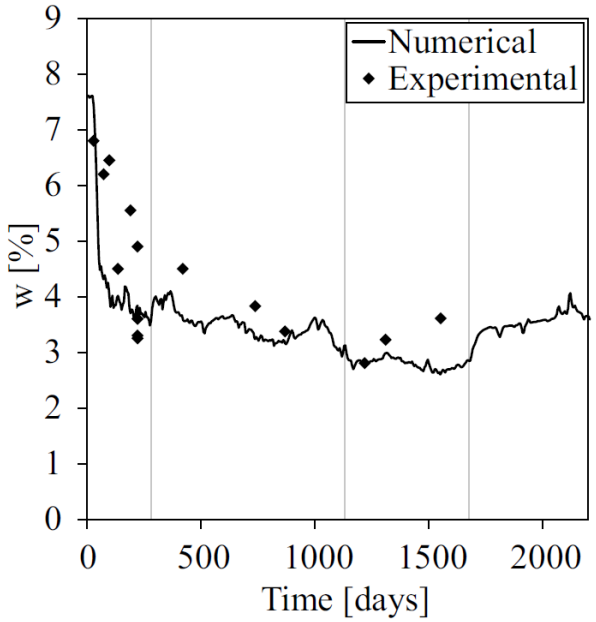

→ Desaturation: overestimation in long term

→ Vapour transfer ($\alpha_v = 10^{-3}$ m/s)

→ Good reproduction at gallery wall

Outline

Conclusions

Better understand, predict, and model the behaviour of the EDZ in partially saturated clay rock, at large scale.

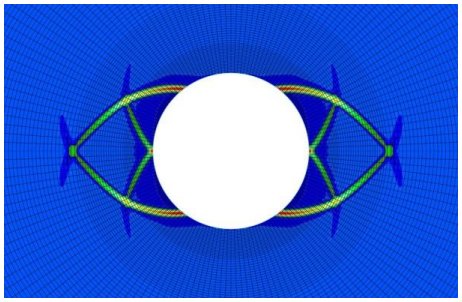

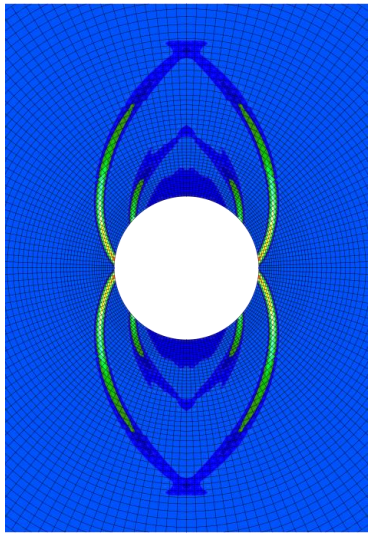

Fracture description

EDZ with strain localisation.

Constitutive models

Mechanics: anisotropy, viscosity.

Coupled: fracture influence on permeability.

Numerical modelling

Shape, extent.

Influence of fracturing, permeability variation, anisotropy.

Water transfer.

Contribution : Provide new elements for the prediction and understanding of the HM behaviour of the EDZ.

Innovations : Fracturing process is predicted on a **large scale** with **shear bands.**
Strain localisation effects are taken into account in **coupled processes** (water flow).

APPENDICES

- Fracturation = 3D problem

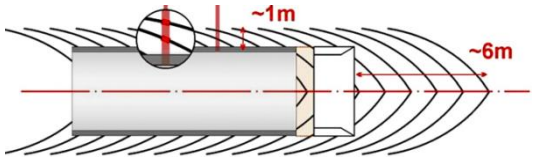

Fractures pattern around a gallery in Boom clay

- Mesh:

Mechanical modelling in 3D state.

Classical FE, no regularisation method.

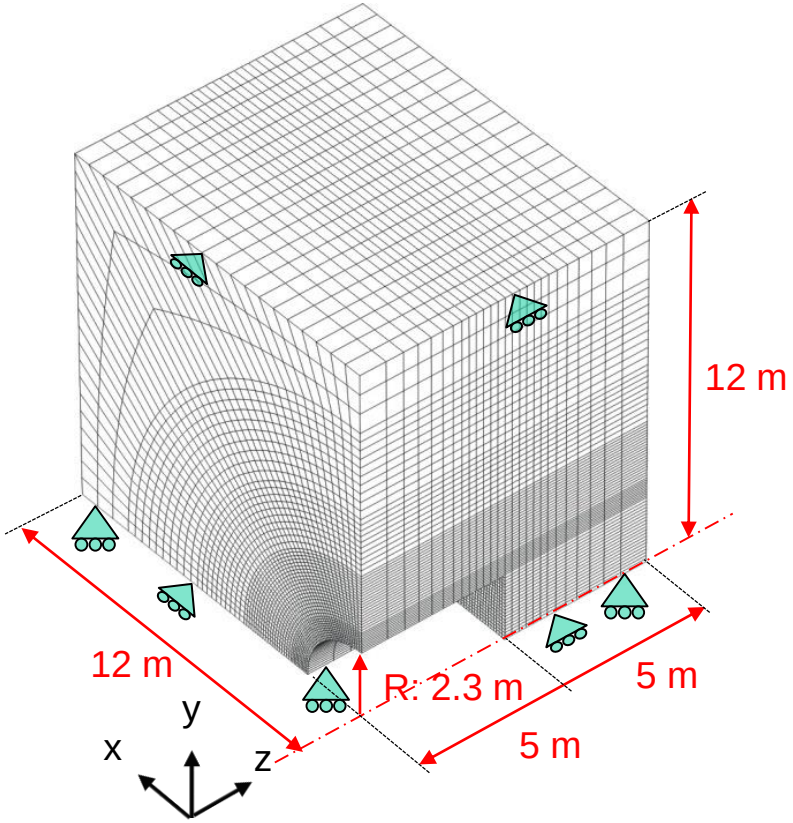

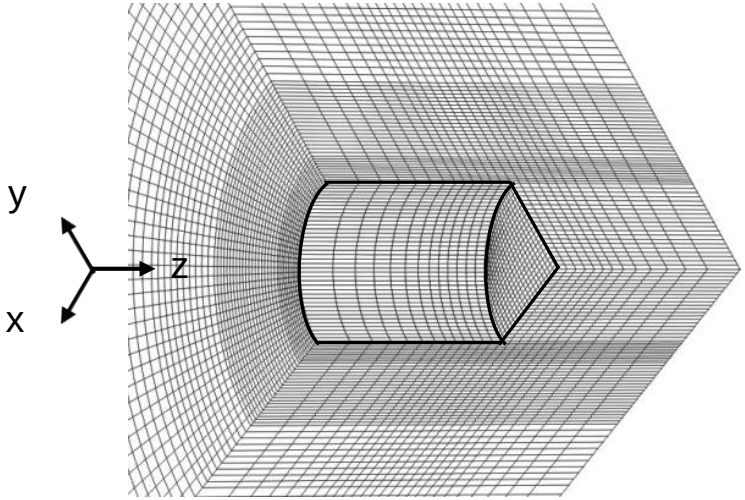

- Localisation zone:

Equivalent deformation ε_{eq} during boring. $\hat{\varepsilon}_{eq} = \sqrt{\frac{2}{3}\hat{\varepsilon}_{ij}\hat{\varepsilon}_{ij}}$

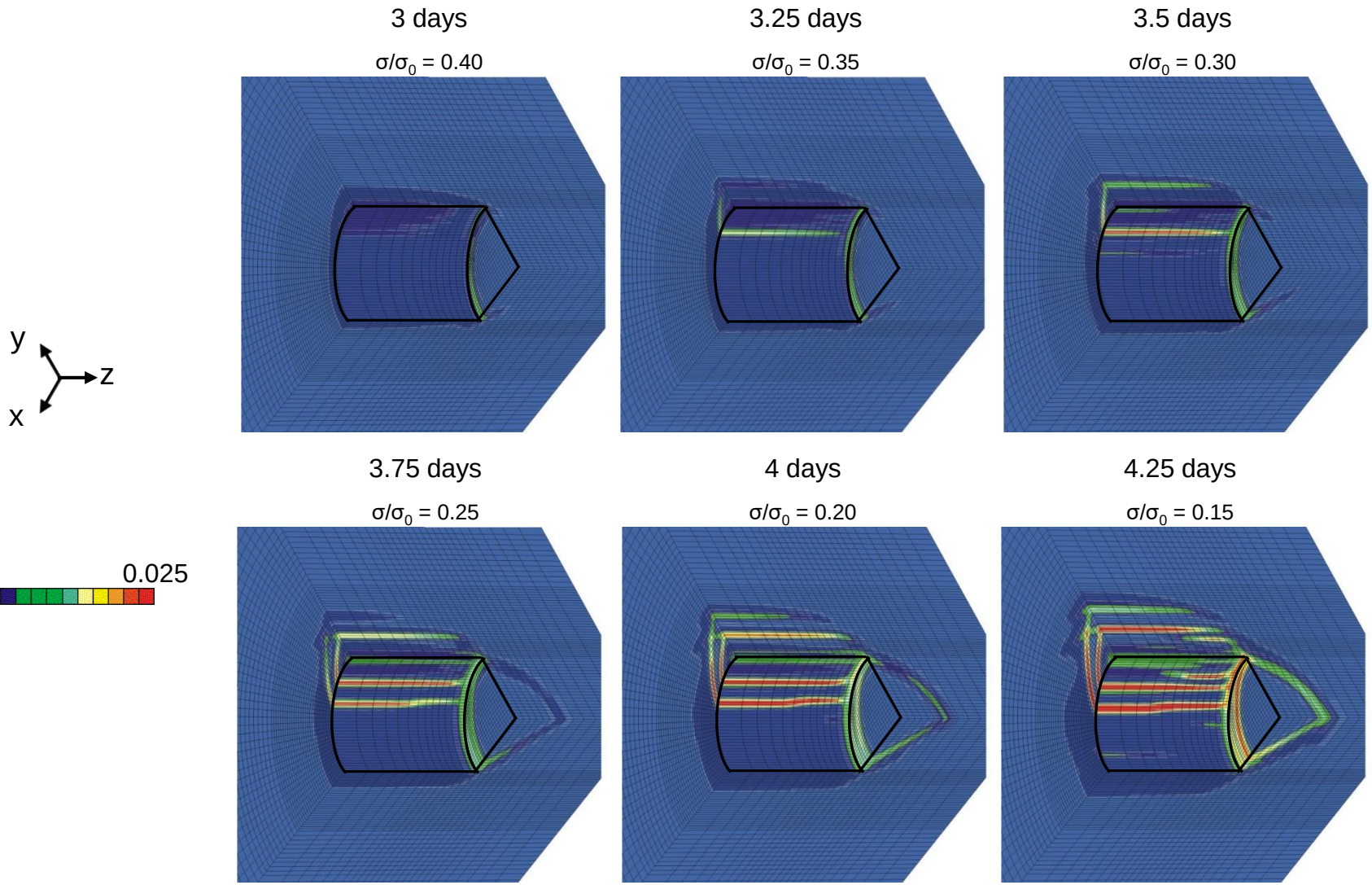

- Localisation zone:

Equivalent deformation ε_{eq} during boring. $\hat{\varepsilon}_{eq} = \sqrt{\frac{2}{3}\hat{\varepsilon}_{ij}\hat{\varepsilon}_{ij}}$

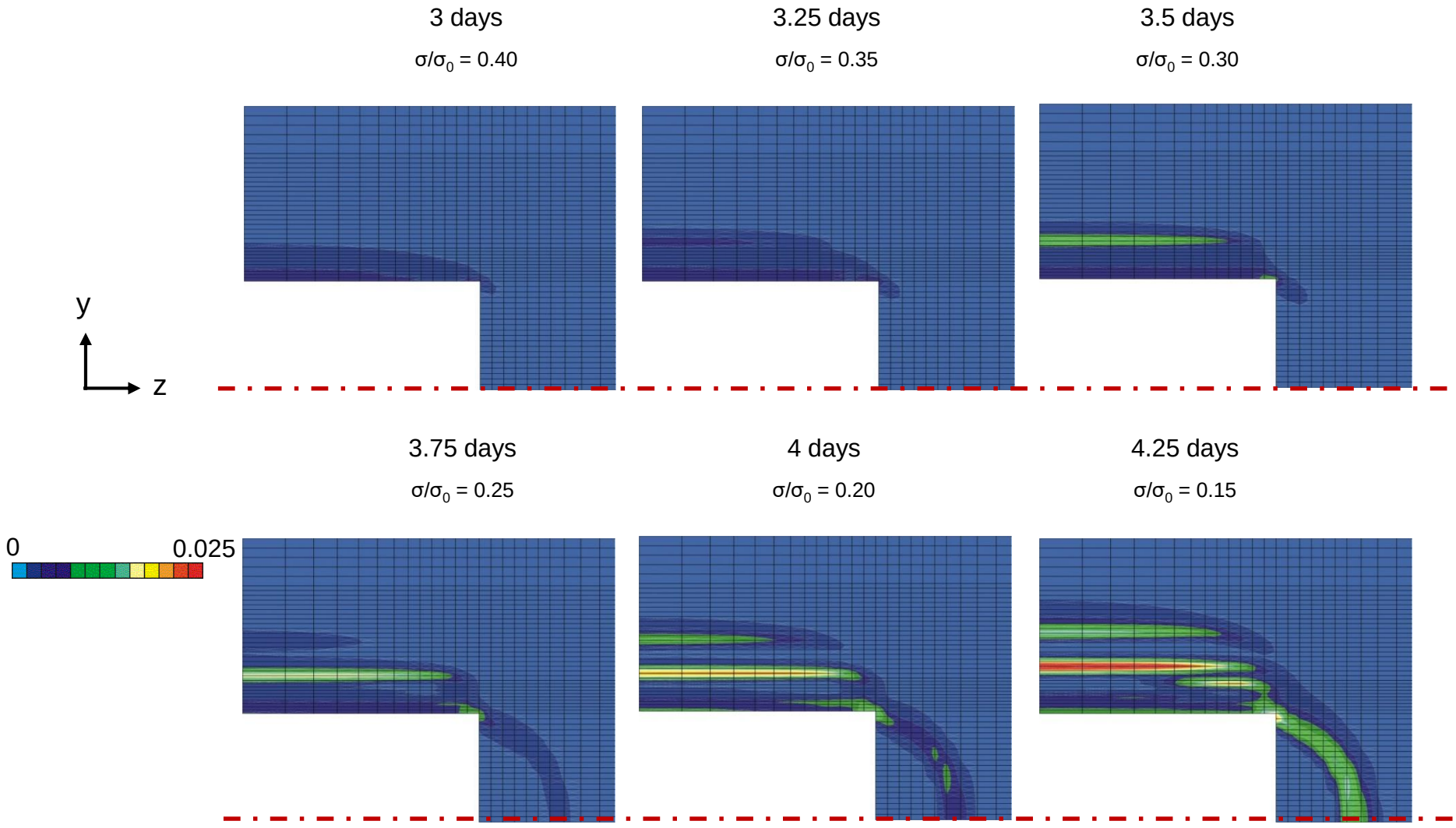

- Localisation zone

Equivalent deformation ε_{eq} - for 4.25 days of excavation (σ/σ_0 = 0.15) :

z<0 : excavation zone

z=0 : gallery front

z>0 : rock mass

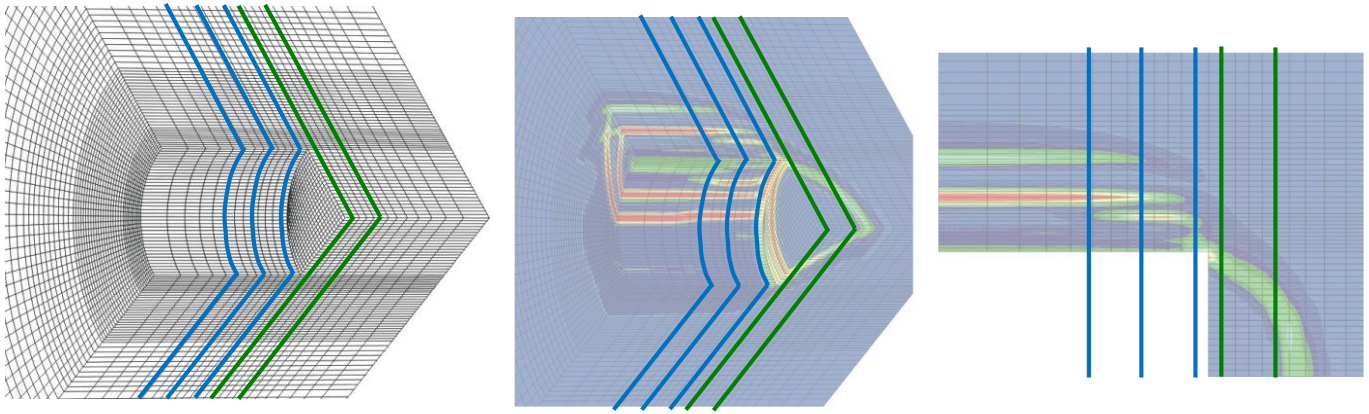

z=-2.25m | z=-1.25m | z=-0.25m | z=+0.25m | z=+1.25m

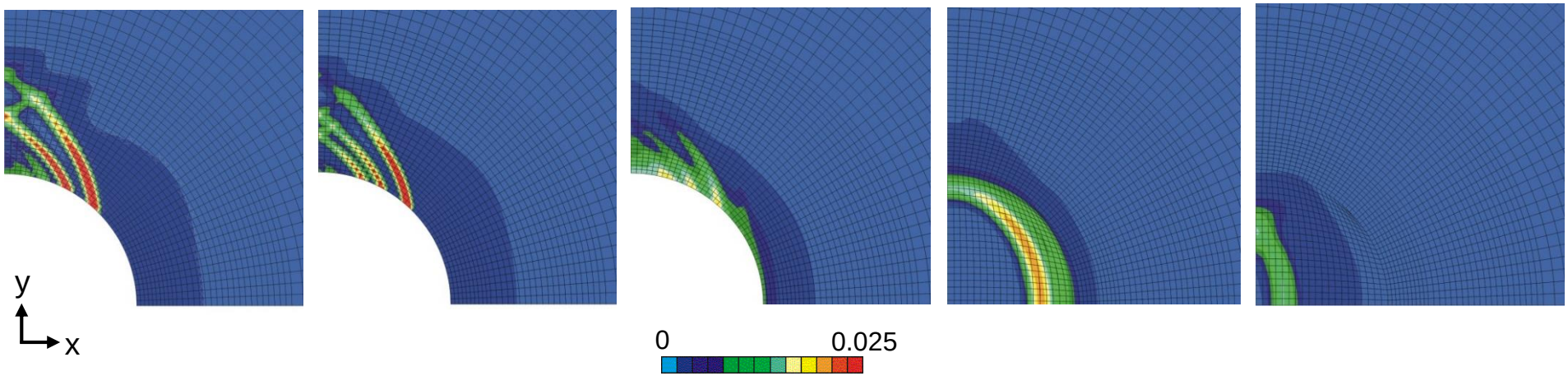

Compressibility influence on shear banding

Biot's coefficient: b=0.6

Total deviatoric strain

Plasticity

1009 days

End of excavation

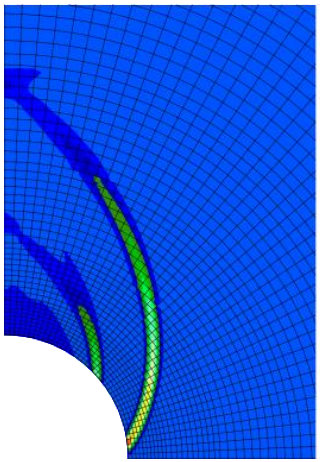

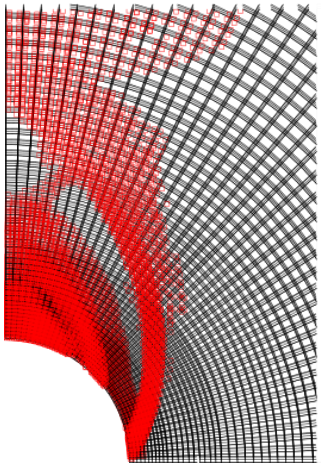

Plasticity

b=0.6

4 days

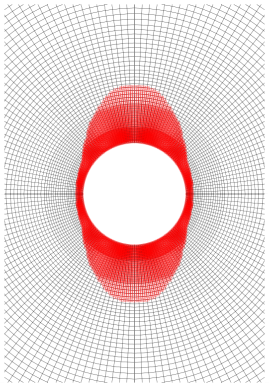

5 days

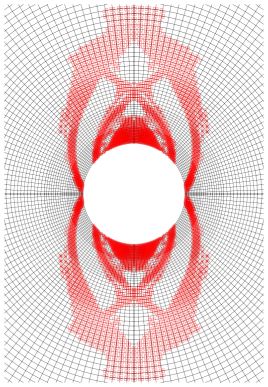

b=1

4 days

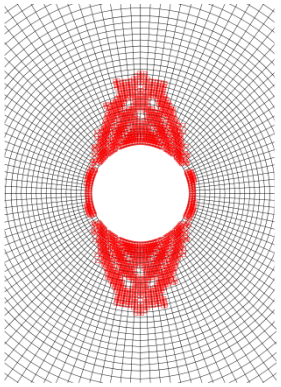

5 days

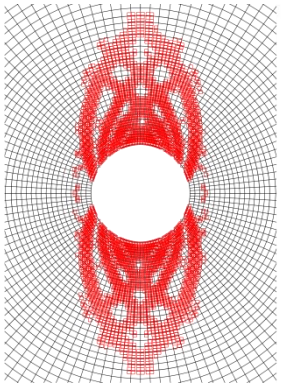

$$\sigma_{ij} = \sigma'_{ij} + b\, S_{r,w}\, p_w\, \delta_{ij}$$

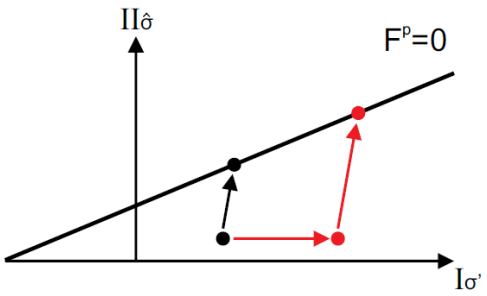

Air ventilation influence on shear banding

- Gallery air ventilation :

Ventilation

100 days 1000 days

Total deviatoric strain

0 0.184

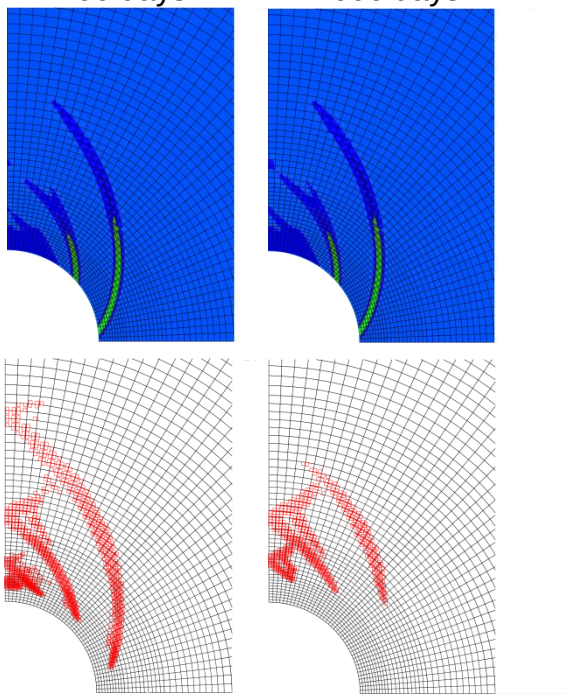

Plasticity

$$\sigma_{ij} = \sigma'_{ij} + b\, S_{r,w}\; p_w\; \delta_{ij}$$

→suction ↑

→σ' ↑

→Elastic unloading

→Inhibition of localisation

→ Restrain ε

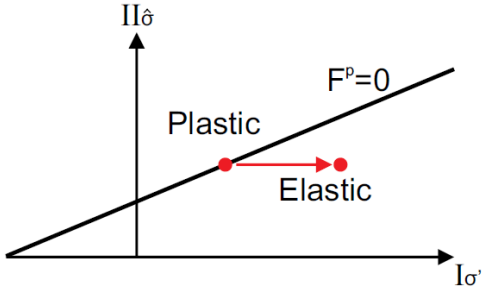

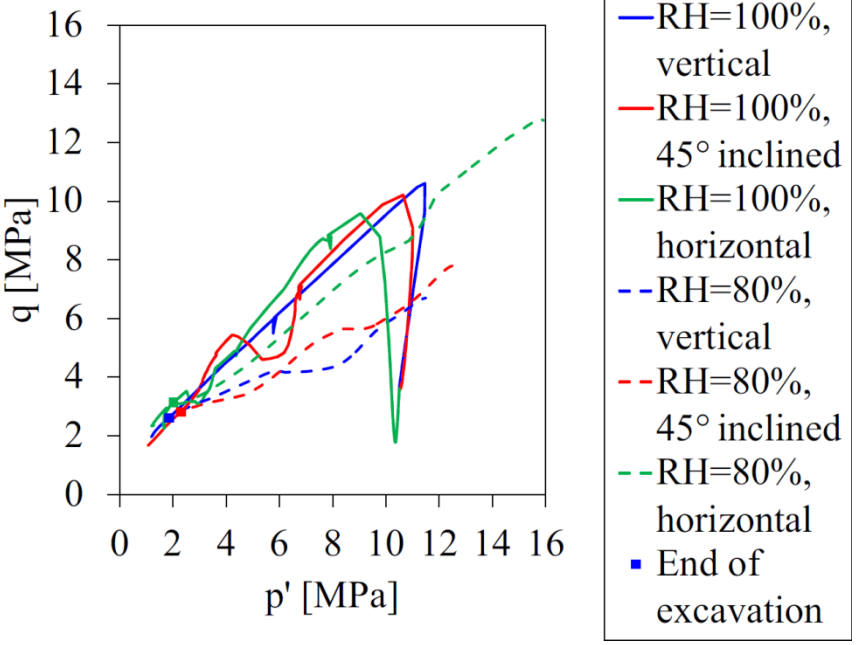

Finite element formulation – 2d gradient model

- Spatial discretisation

Matricial form of balance equations:

$$\int_{\Omega^{\tau 1}} \left[U^{*,\tau 1}_{(x_1,x_2)}\right]^T \left[E^{\tau 1}\right]\left[dU^{\tau 1}_{(x_1,x_2)}\right] d\Omega^{\tau 1} = -\Delta_1^{\tau 1} - \Delta_2^{\tau 1} - \Delta_3^{\tau 1}$$

$\left[dU^{\tau 1}_{(x_1,x_2)}\right]$ vector of the unknown increments of nodal variables

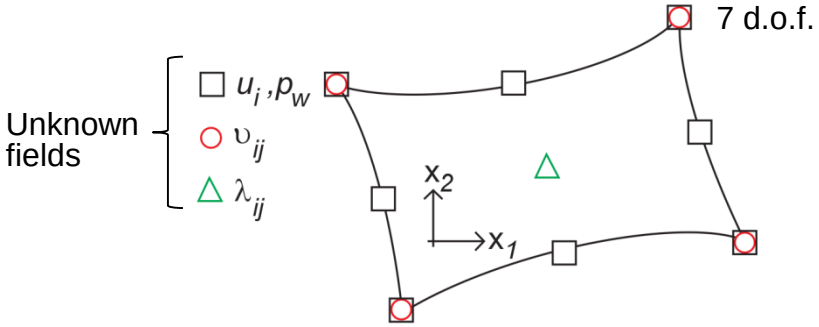

- Element stiffness matrix

Unsaturated condition, $S_{r,w}$

Soild phase compressibility, b

Permeability anisotropy and evolution, $k_{w,ij}$

$$\left[E^{\tau 1}\right]_{25\times 25} = \begin{bmatrix} E^{\tau 1}_{1_{4\times 4}} & 0_{4\times 2} & K^{\tau 1}_{WM_{4\times 3}} & 0_{4\times 8} & 0_{4\times 4} & -I_{4\times 4} \\ G^{\tau 1}_{1_{2\times 4}} & 0_{2\times 2} & G^{\tau 1}_{2_{2\times 3}} & 0_{2\times 8} & 0_{2\times 4} & 0_{2\times 4} \\ K^{\tau 1}_{MW_{3\times 4}} & 0_{3\times 2} & K^{\tau 1}_{WW_{3\times 3}} & 0_{3\times 8} & 0_{3\times 4} & 0_{3\times 4} \\ E^{\tau 1}_{2_{8\times 4}} & 0_{8\times 2} & 0_{8\times 3} & D^{\tau 1}_{8\times 8} & 0_{8\times 4} & 0_{8\times 4} \\ E^{\tau 1}_{3_{4\times 4}} & 0_{4\times 2} & 0_{4\times 3} & 0_{4\times 8} & 0_{4\times 4} & I_{4\times 4} \\ E^{\tau 1}_{4_{4\times 4}} & 0_{4\times 2} & 0_{4\times 3} & 0_{4\times 8} & -I_{4\times 4} & 0_{4\times 4} \end{bmatrix}$$

Second gradient mechanical law – Influence of the elastic modulus

- Second gradient mechanical law

Linear elastic law function

Independent of p_w

$$\tilde{\Sigma}_{ijk} = [D]\frac{\partial \dot{\upsilon}_{ij}}{\partial x_k}$$

Internal length scale

D represents the physical microstructure

$$\begin{bmatrix} \tilde{\Sigma}_{111} \\ \tilde{\Sigma}_{112} \\ \tilde{\Sigma}_{121} \\ \tilde{\Sigma}_{122} \\ \tilde{\Sigma}_{211} \\ \tilde{\Sigma}_{212} \\ \tilde{\Sigma}_{221} \\ \tilde{\Sigma}_{222} \end{bmatrix} = D \begin{bmatrix} 1 & 0 & 0 & 0 & 0 & \frac{1}{2} & \frac{1}{2} & 0 \\ 0 & \frac{1}{2} & \frac{1}{2} & 0 & -\frac{1}{2} & 0 & 0 & \frac{1}{2} \\ 0 & \frac{1}{2} & \frac{1}{2} & 0 & -\frac{1}{2} & 0 & 0 & \frac{1}{2} \\ 0 & 0 & 0 & 1 & 0 & -\frac{1}{2} & -\frac{1}{2} & 0 \\ 0 & -\frac{1}{2} & -\frac{1}{2} & 0 & 1 & 0 & 0 & 0 \\ \frac{1}{2} & 0 & 0 & -\frac{1}{2} & 0 & \frac{1}{2} & \frac{1}{2} & 0 \\ \frac{1}{2} & 0 & 0 & -\frac{1}{2} & 0 & \frac{1}{2} & \frac{1}{2} & 0 \\ 0 & \frac{1}{2} & \frac{1}{2} & 0 & 0 & 0 & 0 & 1 \end{bmatrix} \begin{bmatrix} \frac{\partial \dot{\upsilon}_{11}}{\partial x_1} \\ \frac{\partial \dot{\upsilon}_{11}}{\partial x_2} \\ \frac{\partial \dot{\upsilon}_{12}}{\partial x_1} \\ \frac{\partial \dot{\upsilon}_{12}}{\partial x_2} \\ \frac{\partial \dot{\upsilon}_{21}}{\partial x_1} \\ \frac{\partial \dot{\upsilon}_{21}}{\partial x_2} \\ \frac{\partial \dot{\upsilon}_{22}}{\partial x_1} \\ \frac{\partial \dot{\upsilon}_{22}}{\partial x_2} \end{bmatrix}$$

Plasticity

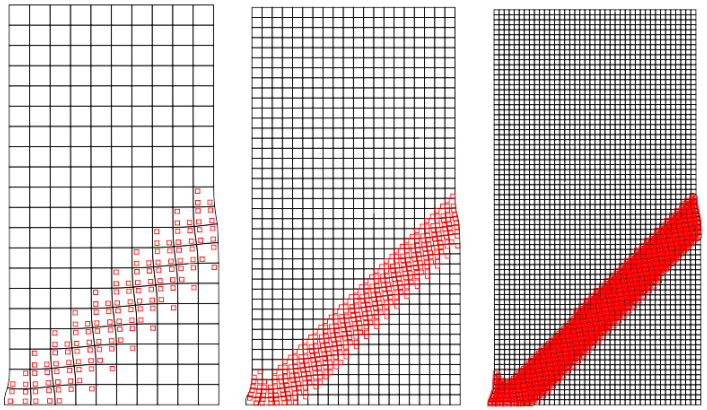

Total deviatoric strain $\hat{\varepsilon}_{eq} = \sqrt{\frac{2}{3}\hat{\varepsilon}_{ij}\hat{\varepsilon}_{ij}}$

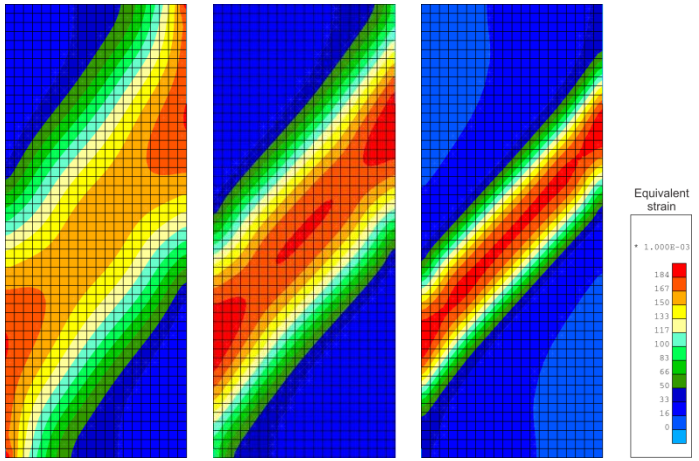

D = 80 N D = 20 N D = 5 N

→ D should be evaluated based on experimental measurements

→ Better numerical precision if a few elements compose the shear band width

→ Large scale …

Influence of mechanical anisotropy

Cross-anisotropic elasticity

Linear elasticity (5 param.)

$$d\varepsilon_{ij}^{e} = D_{ijkl}^{e} d\sigma_{kl}^{'} \qquad E_{//}, E_{\perp}, \nu_{////}, \nu_{//\perp}, G_{//\perp}$$

$$\frac{\nu_{//\perp}}{E_{//}} = \frac{\nu_{\perp//}}{E_{\perp}} \qquad G_{////} = \frac{E_{//}}{2(1+\nu_{////})}$$

$$D_{ijkl}^{e} = \begin{bmatrix} \frac{1}{E_{//}} & -\frac{\nu_{\perp//}}{E_{\perp}} & -\frac{\nu_{////}}{E_{//}} & & & \\ -\frac{\nu_{//\perp}}{E_{//}} & \frac{1}{E_{\perp}} & -\frac{\nu_{//\perp}}{E_{//}} & & & \\ -\frac{\nu_{////}}{E_{//}} & -\frac{\nu_{\perp//}}{E_{\perp}} & \frac{1}{E_{//}} & & & \\ & & & \frac{1}{2G_{//\perp}} & & \\ & & & & \frac{1}{2G_{////}} & \\ & & & & & \frac{1}{2G_{\perp//}} \end{bmatrix}$$

Biot's coefficients

$$b_{ij} = \delta_{ij} - \frac{C_{ijkk}^{e}}{3K_s} \qquad b_{ij} = \begin{bmatrix} b_{//} & & \\ & b_{\perp} & \\ & & b_{//} \end{bmatrix}$$

$$b_{//} = 1 - \frac{1+\nu_{////}+\nu_{////}\nu_{\perp//}+\nu_{\perp//}}{3E_{//}E_{\perp}\Upsilon K_s}$$

$$b_{\perp} = 1 - \frac{1-\nu_{////}^{2}+2\nu_{//\perp}+2\nu_{//\perp}\nu_{////}}{3E_{//}E_{//}\Upsilon K_s}$$

Micro-homogeneity and micro-isotropy assumptions (Cheng, 1997) for which K_s is homogeneous and isotropic at grains scale.

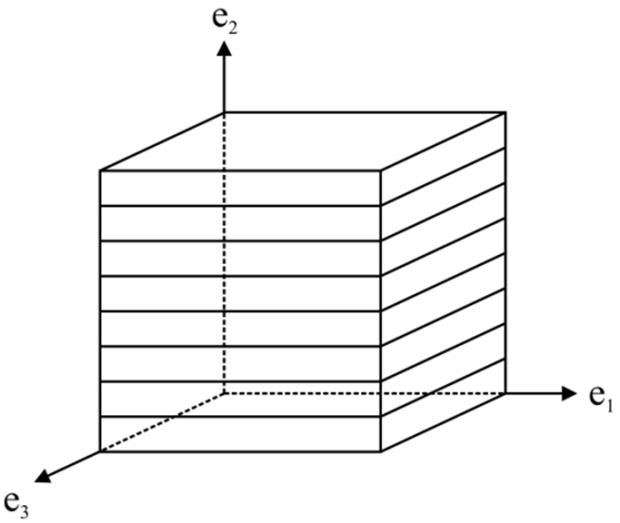

Influence of mechanical anisotropy

Anisotropic plasticity with fabric tensor

Cohesion anisotropy with fabric tensor.

c_0 is the projection of the tensor on a generalised unit loading vector :

$$c_0 = a_{ij}\, l_i\, l_j \qquad l_i = \sqrt{\frac{\sigma'^2_{i1} + \sigma'^2_{i2} + \sigma'^2_{i3}}{\sigma'_{ij}\sigma'_{ij}}} \qquad \|l_i\| = 1$$

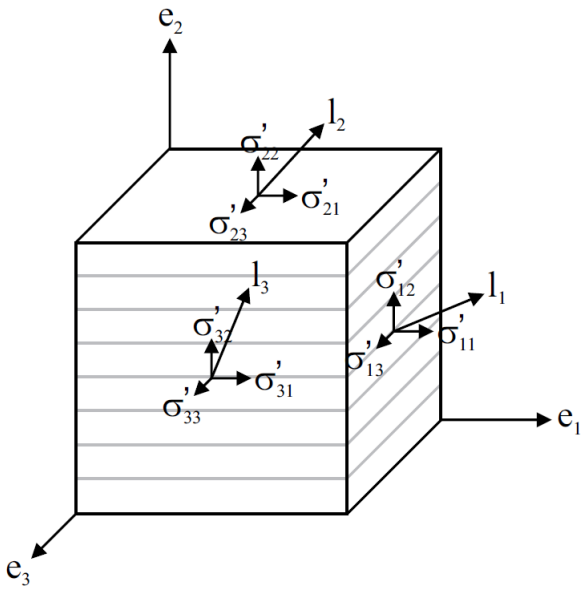

Deviatoric part:

$$\hat{a}_{ij} = a_{ij} - \bar{c}\,\delta_{ij} \quad , \quad \bar{c} = \frac{a_{ii}}{3}$$

$$A_{ij} = \frac{\hat{a}_{ij}}{\bar{c}} \quad , \quad A_{ii} = \hat{a}_{ii} = 0 \qquad \Rightarrow \qquad c_0 = \bar{c}\left(1 + A_{ij}\, l_i\, l_j\right)$$

Generalisation with higher order tensor:

$$c_0 = \bar{c}\left(1 + A_{ij}\, l_i\, l_j + b_1\left(A_{ij}\, l_i\, l_j\right)^2 + b_2\left(A_{ij}\, l_i\, l_j\right)^3 + \ldots\right)$$

Orthotropy:

$$A_{ij} = \begin{bmatrix} A_{11} & 0 & 0 \\ 0 & A_{22} & 0 \\ 0 & 0 & A_{33} \end{bmatrix} \qquad \Rightarrow \qquad A_{ij}\, l_i\, l_j = A_{11} l_1^2 + A_{22} l_2^2 + A_{33} l_3^2$$

Cross-anisotropy:

$$A_{ij} = \begin{bmatrix} A_{////} & 0 & 0 \\ 0 & A_{\perp\perp} & 0 \\ 0 & 0 & A_{////} \end{bmatrix} \qquad \Rightarrow \qquad A_{ij}\, l_i\, l_j = A_{////}\left(1 - 3 l_2^2\right)$$

$$A_{\perp\perp} = -2\, A_{////} \quad , \quad \|l_i\| = 1$$

$$c_0 = \bar{c}\left(1 + A_{////}\left(1 - 3 l_2^2\right) + b_1 A_{////}^2\left(1 - 3 l_2^2\right)^2 + b_2 A_{////}^3\left(1 - 3 l_2^2\right)^3 + \ldots\right)$$

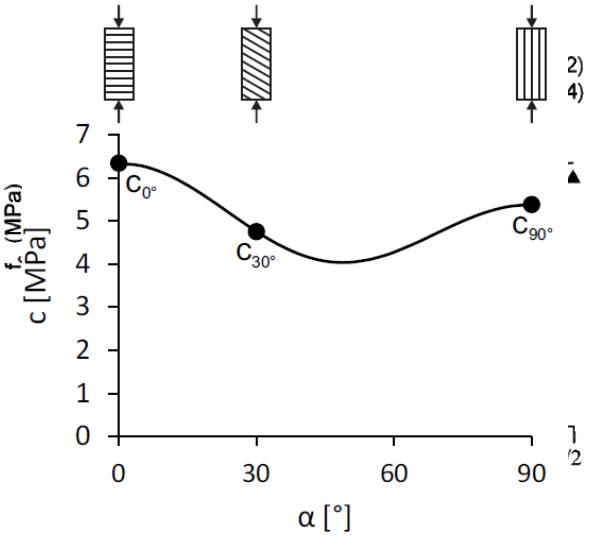

Viscosity

Time-dependent plastic strain, delayed plastic deformation
Progressive evolution of the material microstructure or to mechanical properties degradation (damage)

$$\dot{\varepsilon}_{ij} = \dot{\varepsilon}^{e}_{ij} + \dot{\varepsilon}^{p}_{ij} + \dot{\varepsilon}^{vp}_{ij}$$

Viscoplastic loading surface and potential surface:

$$F^{vp} \equiv \sqrt{3}\, II_{\hat{\sigma}} - \alpha^{vp}\, g(\beta)\, R_c \sqrt{A^{vp}\left(C^{vp} + \frac{I_{\sigma'}}{3R_c}\right)} = 0$$

$$G^{vp} \equiv \sqrt{3}\, II_{\hat{\sigma}} - \left(\alpha^{vp} - \beta^{vp}\right) g(\beta)\, R_c \left(C^{vp} + \frac{I_{\sigma'}}{3R_c}\right) = 0$$

$$\dot{\varepsilon}^{vp}_{ij} = \gamma \left\langle \frac{F^{vp}}{R_c} \right\rangle^{N} \frac{\partial G^{vp}}{\partial \sigma'_{ij}}$$

Delayed viscoplastic hardening function:

$$\alpha^{vp} = \alpha^{vp}_0 + \left(1 - \alpha^{vp}_0\right) \frac{\varepsilon^{vp}_{eq}}{B^{vp} + \varepsilon^{vp}_{eq}}$$

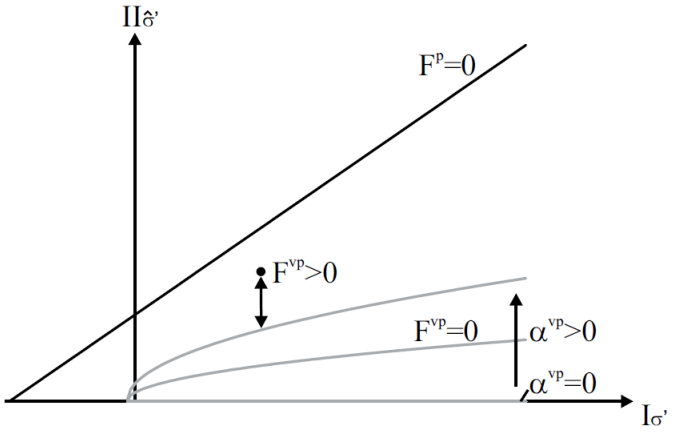

Permeability evolution and water transfer

- Reproduction at the end of excavation

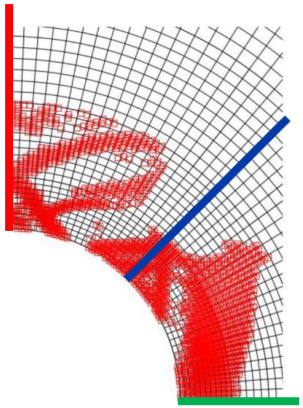

$$k_{w,ij} = k_{w,ij,0}\left(1+\beta\langle\gamma\rangle^3\right)$$

(a) Volumetric strain

$$\gamma = \varepsilon_v = \varepsilon_{ii}/3$$

(b) Equivalent deviatoric total strain

$$\gamma = \hat{\varepsilon}_{eq} = \sqrt{\frac{2}{3}\hat{\varepsilon}_{ij}\hat{\varepsilon}_{ij}}$$

(c) Equivalent deviatoric plastic strain

$$\gamma = \hat{\varepsilon}^p_{eq} = \sqrt{\frac{2}{3}\hat{\varepsilon}^p_{ij}\hat{\varepsilon}^p_{ij}}$$

(d) Plastic strain and a part of the elastic one

$$k_{w,ij} = k_{w,ij,0}\left(1+\beta\left\langle YI - YI^{thr}\right\rangle\hat{\varepsilon}_{eq}{}^3\right)$$

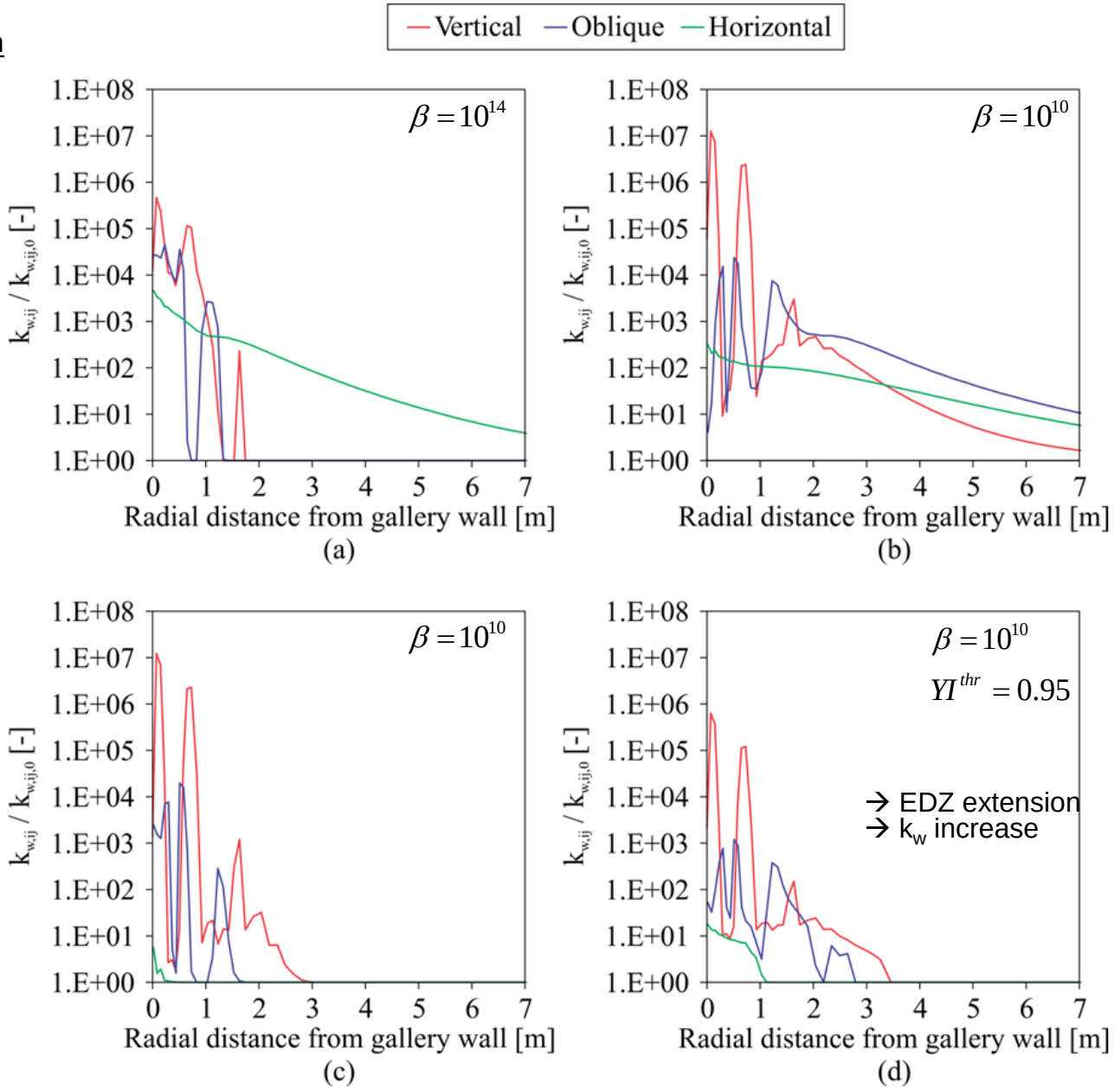

Permeability evolution and water transfer

- Drainage / p_w reproduction

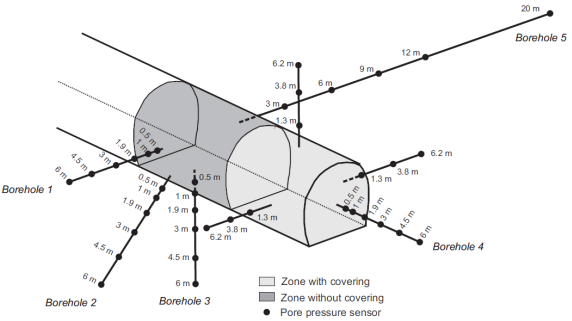

— Numerical - - Experimental

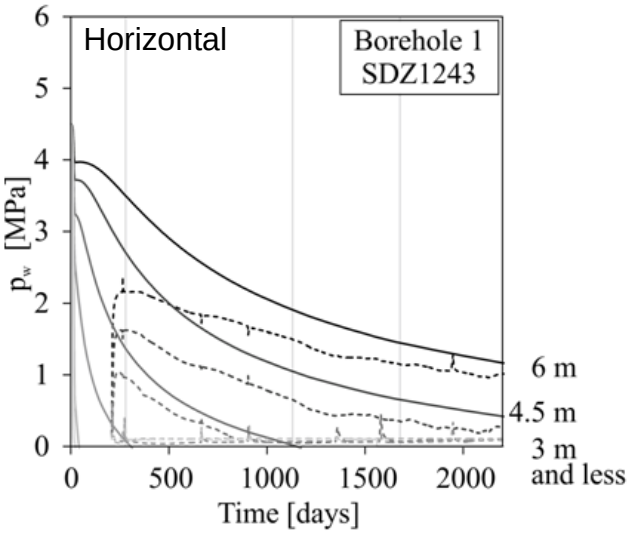

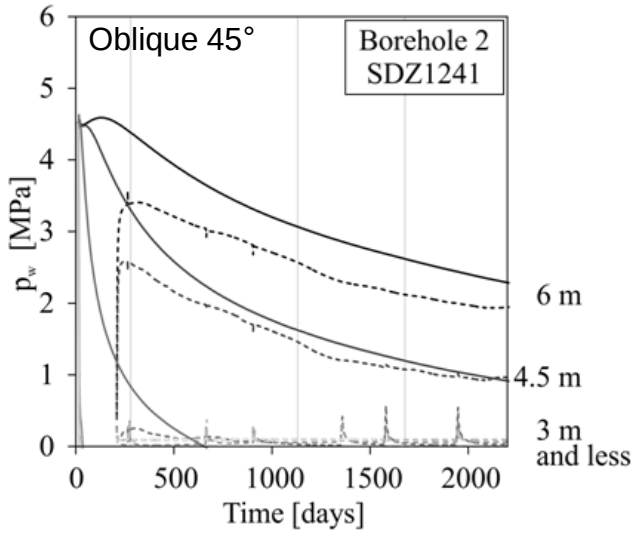

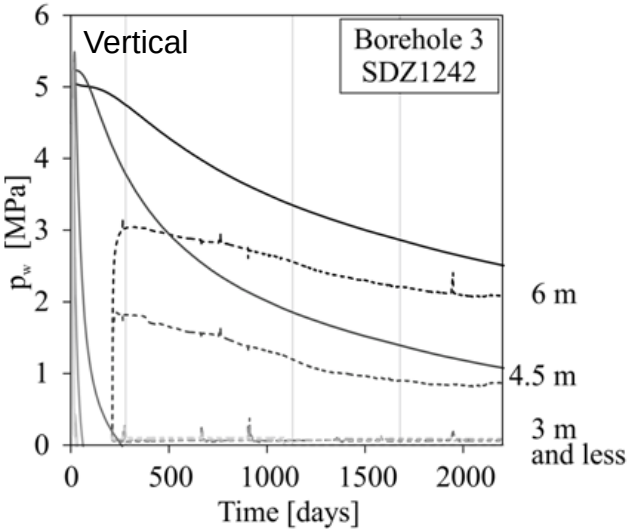

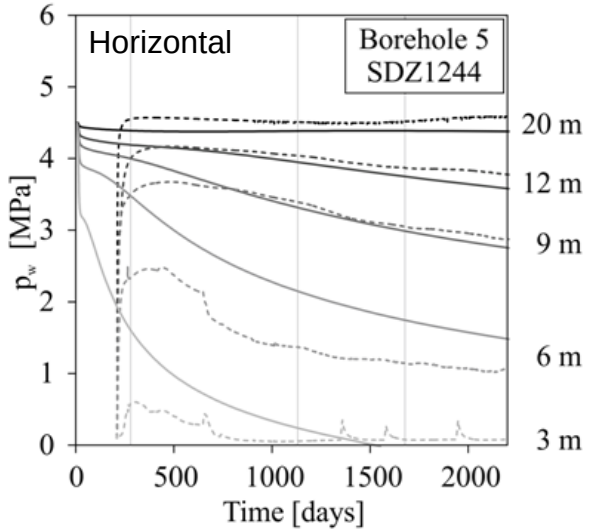

$\alpha_v = 10^{-3}$ m/s

→ Good matching

→ HM effect - $k_{w,h} > k_{w,v}$

Permeability evolution and water transfer

- Desaturation EDZ / w reproduction

At gallery wall

→ Low vertical drainage

→ $k_{w,h} > k_{w,v}$: $k_{w,h/v} = 4\ 10^{-20} / 1.33\ 10^{-20}$ [m²]

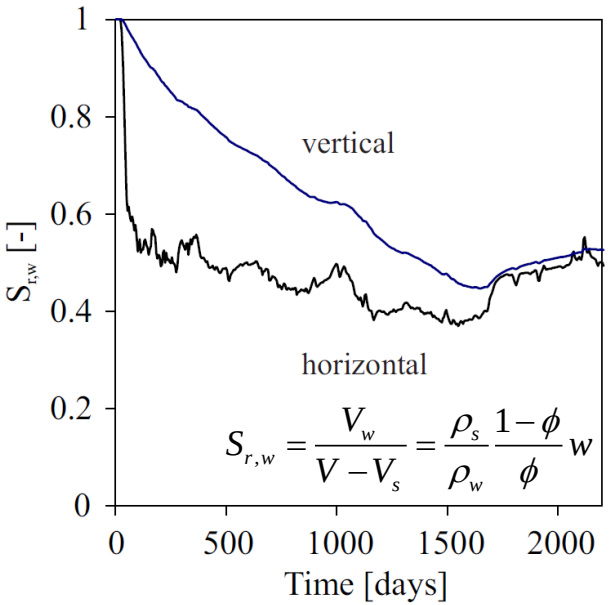

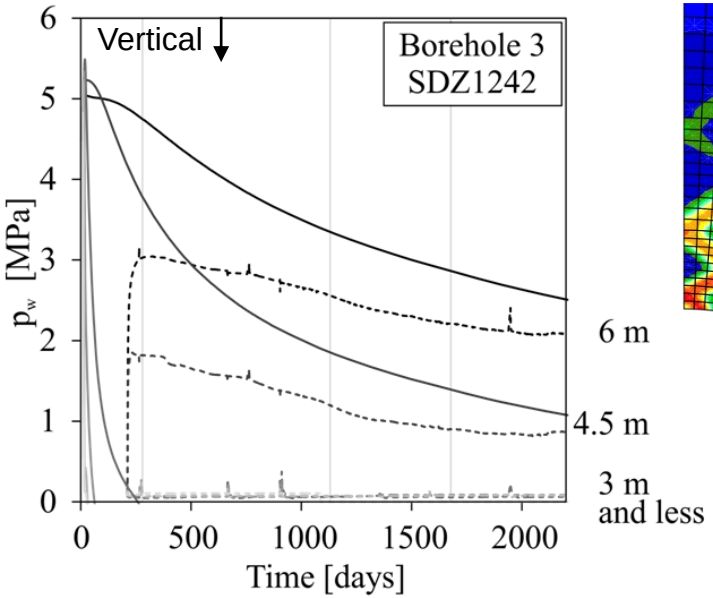

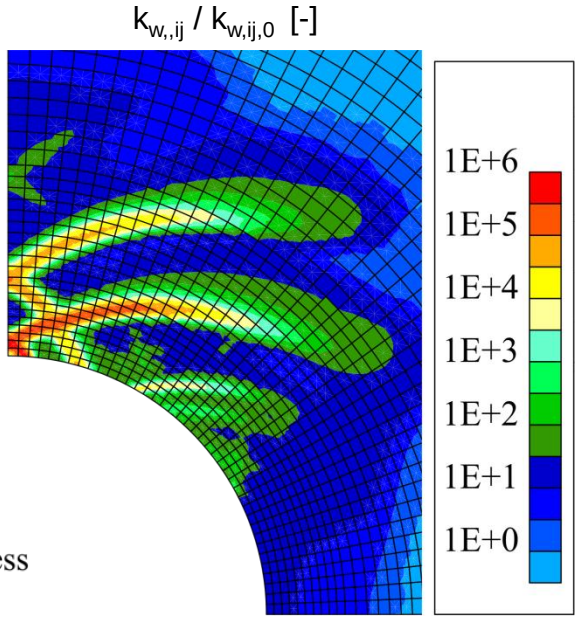

Mechanical anisotropy

- Convergence

Total deviatoric strain

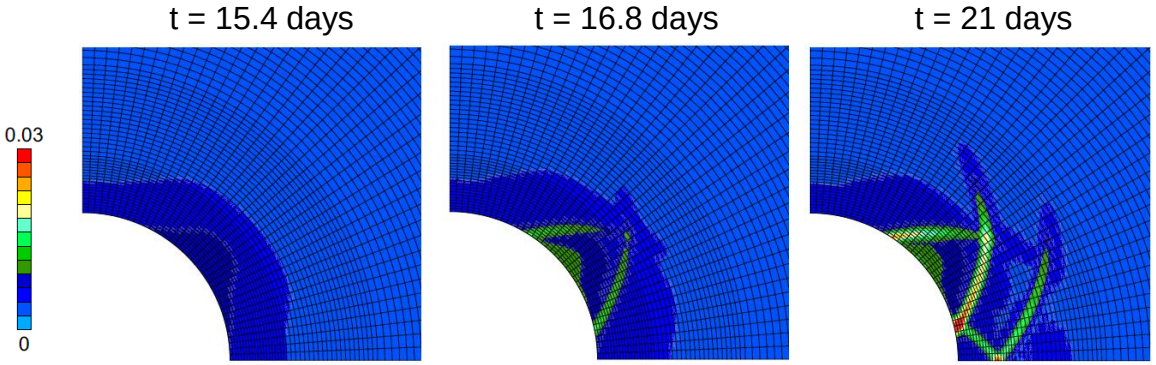

Velocity norm $\| v \| = \sqrt{v_x^2 + v_y^2}$

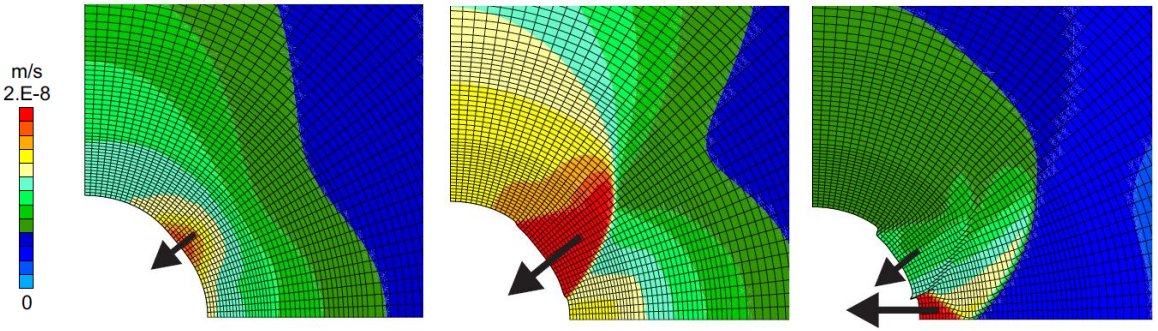

Diametrical convergence

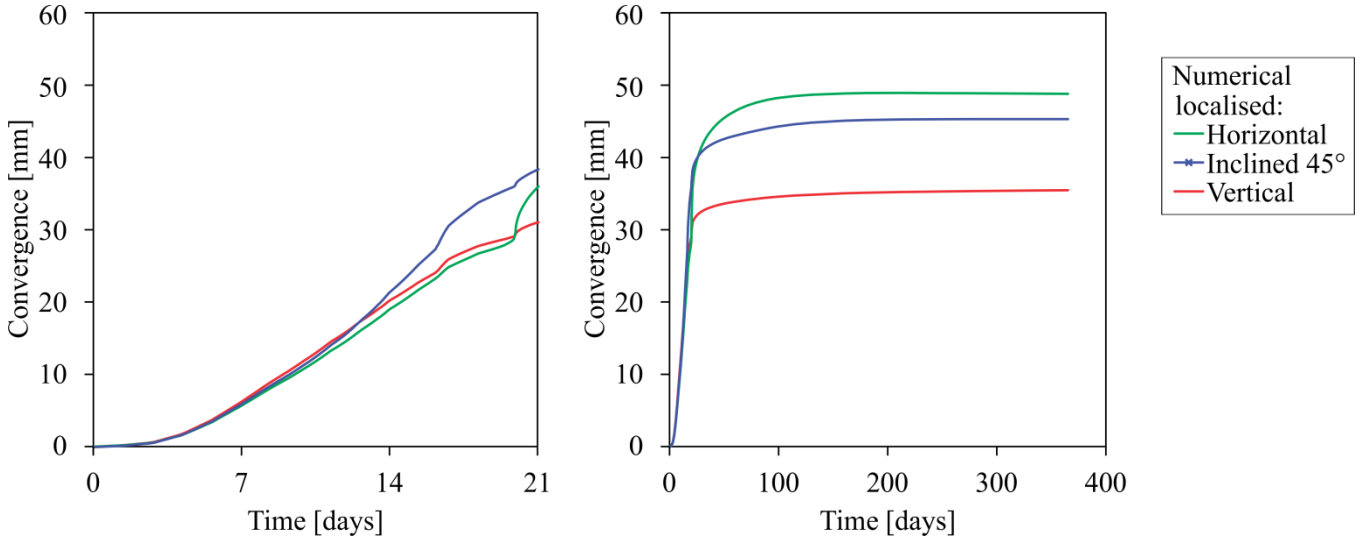

Kinetics of drying process – Mixed boundary condition

- Non-classical mixed boundary condition

Progressive thermodynamic equilibrium by vapour transfer.
Vapour transfer in a boundary layer.

- Non-classical mixed boundary condition

Liquid water + water vapour

$$\bar{q}_w = \bar{S} + \bar{E}$$

- Seepage flow :

$$\begin{cases} \bar{S} = K^{pen}\,(p_w^{\Gamma} - p_{atm})^2 & \text{if } p_w^{\Gamma} \geq p_w^{air} \text{ and } p_w^{\Gamma} \geq p_{atm} \\ \bar{S} = 0 & \textit{otherwise} \end{cases}$$

- Evaporation flow :
(Nasrallah and Perre, 1988)

$$\bar{E} = \alpha_v\,(\rho_v^{\Gamma} - \rho_v^{air})$$

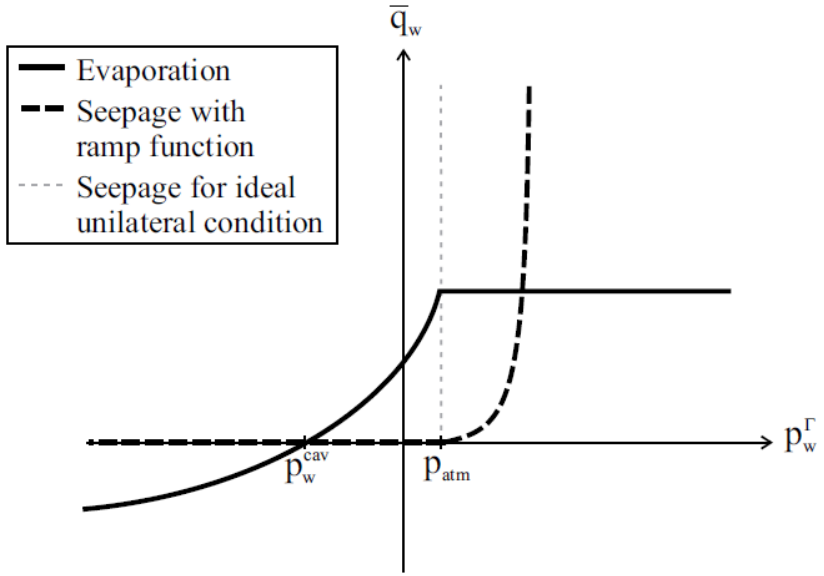

Evaporation and seepage flows at gallery wall for a constant air ventilation (Gerard et al., 2008).

Kinetics of drying process – Water vapour transfer

Drying test : saline solutions (control vapour phase & RH), or convective drying tests

Drying flux curve:

Thermo-hydraulic process and exchanges in a boundary layer.

1. Preheating
2. Constant flux : heat totally used for water evaporation, saturated boundary layer, external conditions (RH, T, v).
3. Decrease of the flow : internal resistances restrict the water outflow, desaturation of the boundary layer

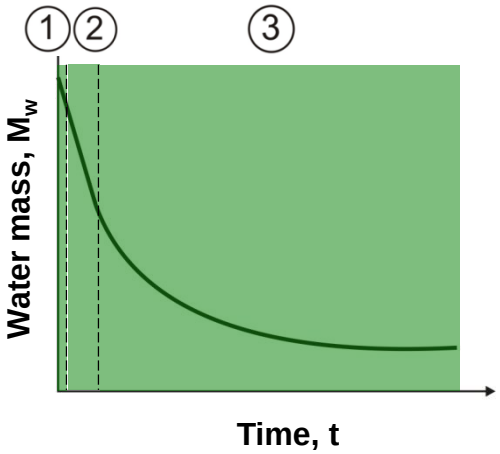

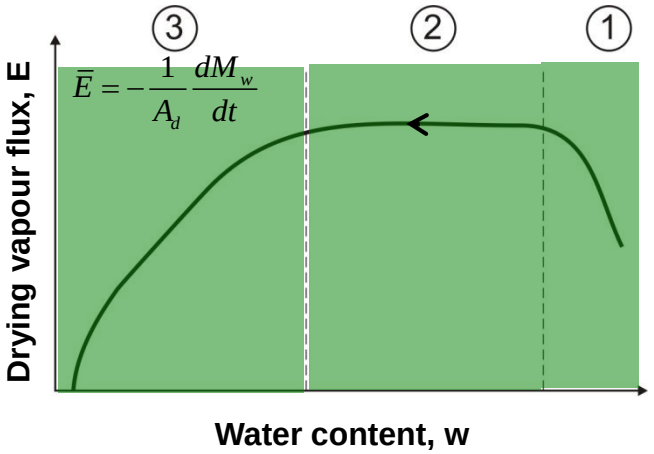

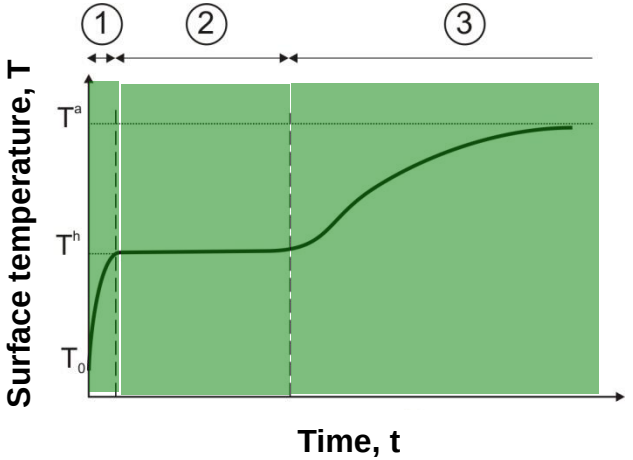

$$\bar{E} = \alpha_v \left(\rho_v^{\Gamma} - \rho_v^{air} \right)$$

$$\alpha_v = \frac{\bar{E}_{\max}}{\rho_v^{\Gamma} - \rho_v^{air}} = \frac{\max\left(-\frac{1}{A_d}\frac{dM_w}{dt} \right)}{\rho_v^{0,\Gamma}(T^h) - RH\,\rho_v^{0,air}(T^a)}$$

→ α_v depends on external drying conditions (RH, T, v)

Gallery excavation modelling for anisotropic initial stress state

Gallery // to σ_h

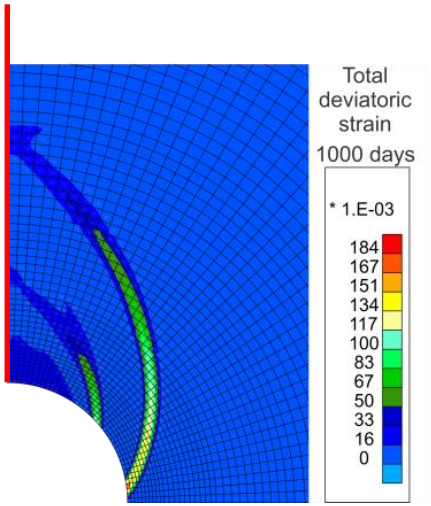

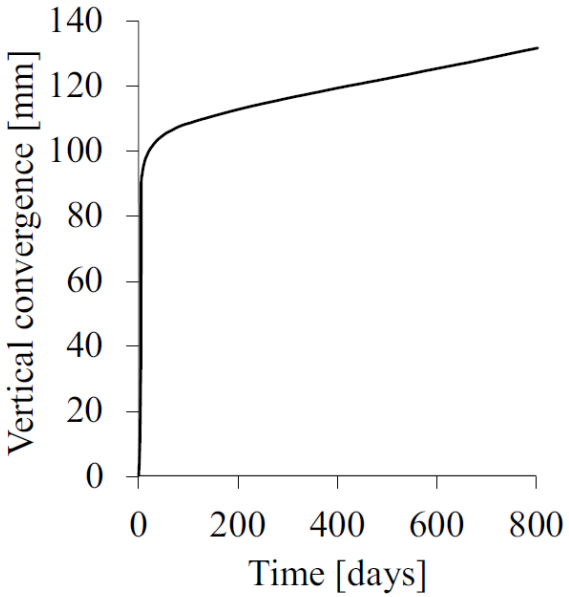

Vertical cross-section

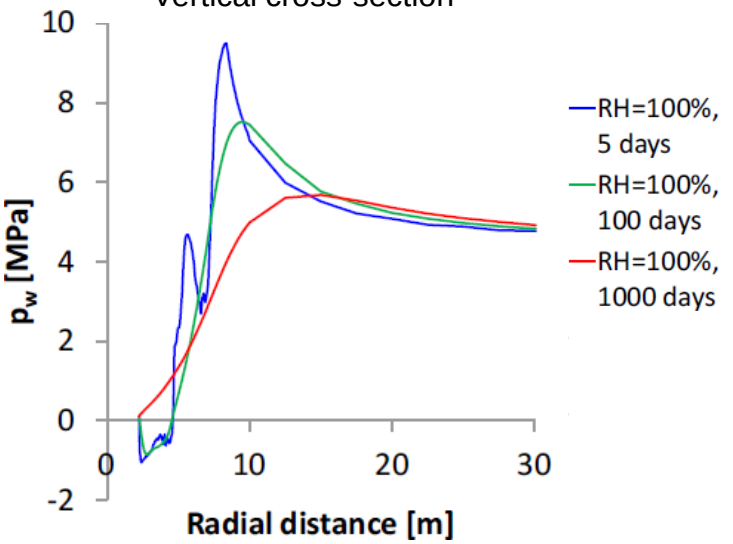

Close to gallery wall:

Strong effect of the localisation bands

σ^r=cst, $p_w\uparrow$, $\sigma'\downarrow$, $\varepsilon^{pl}\uparrow$ (on the yield surface)

Convergence keep increasing

In the vertical: similar

Mine-by experiment

- Displacements

Andra's URL

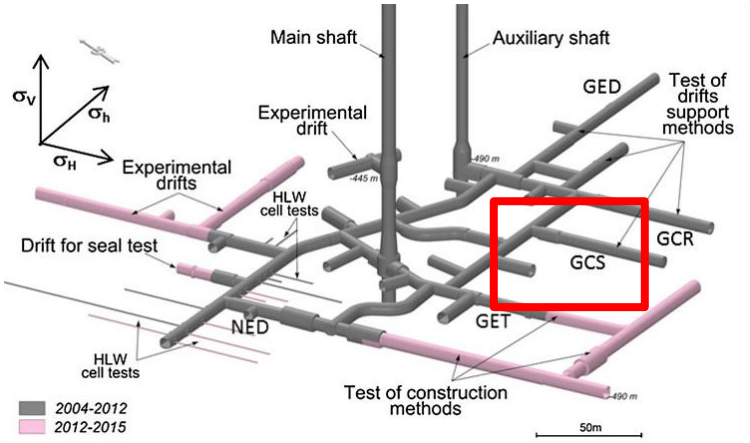

Mine-by experiment

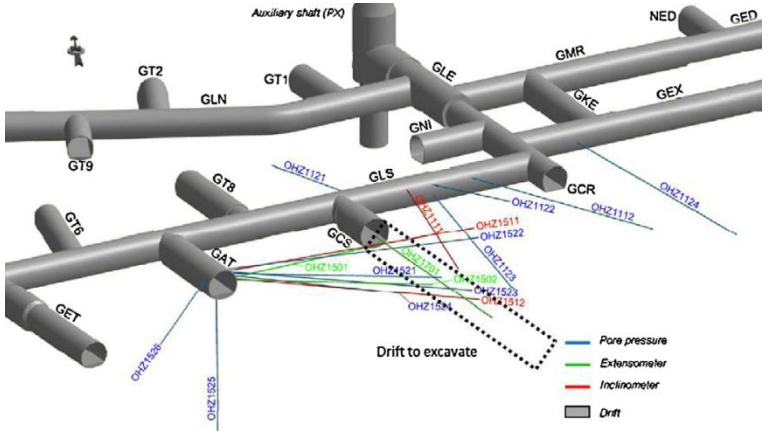

Borehole – extensometers and pore pressure

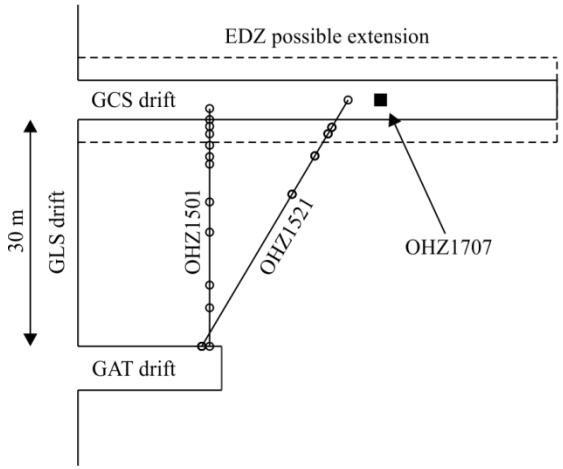

→ Characterise the displacements in the rock mass

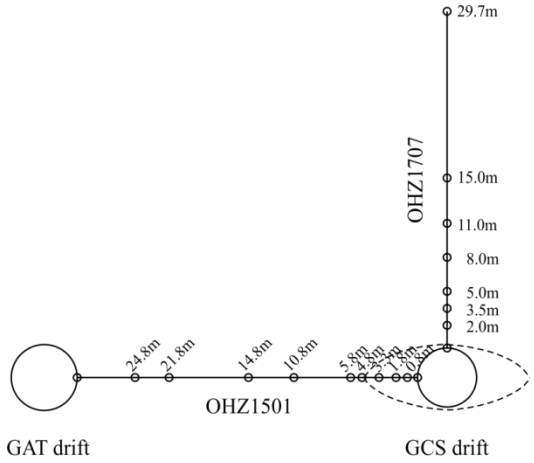

Mine-by experiment

- Displacements

Viscosity based on **creep tests**

Horizontal

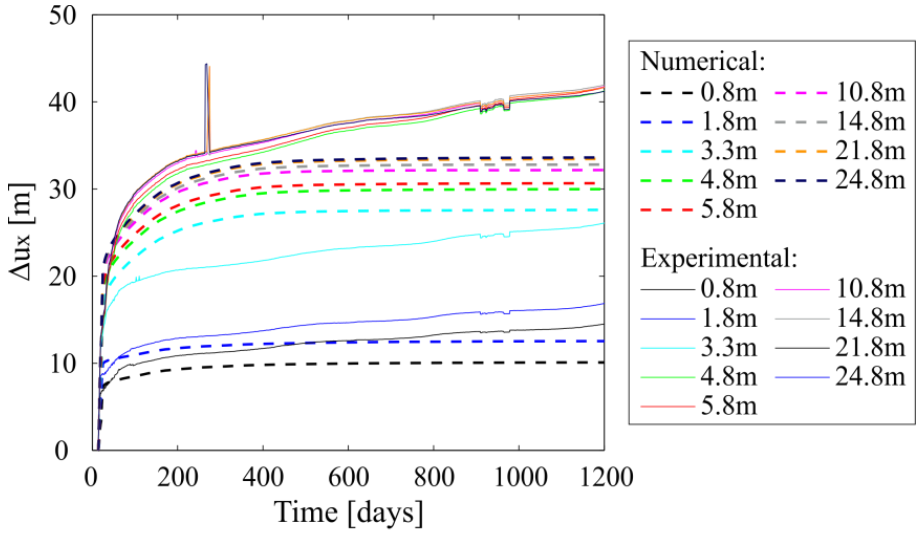

Vertical

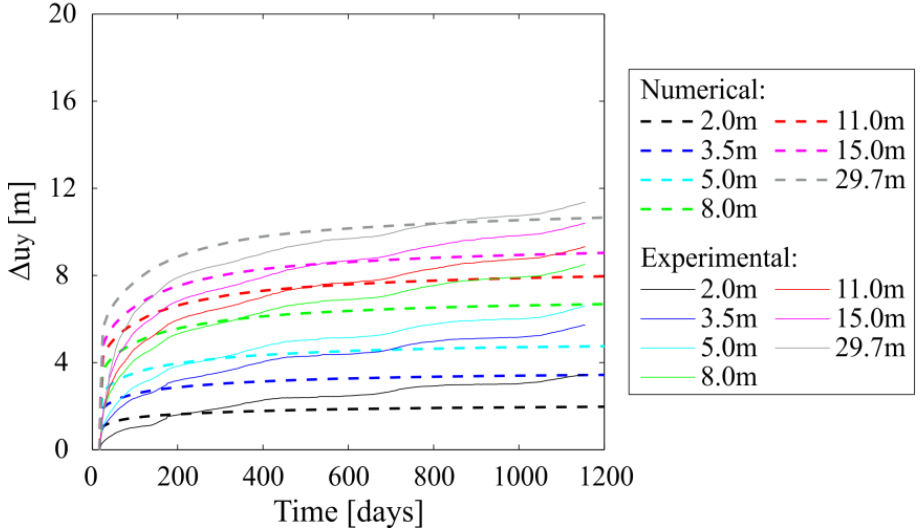

- Convergence

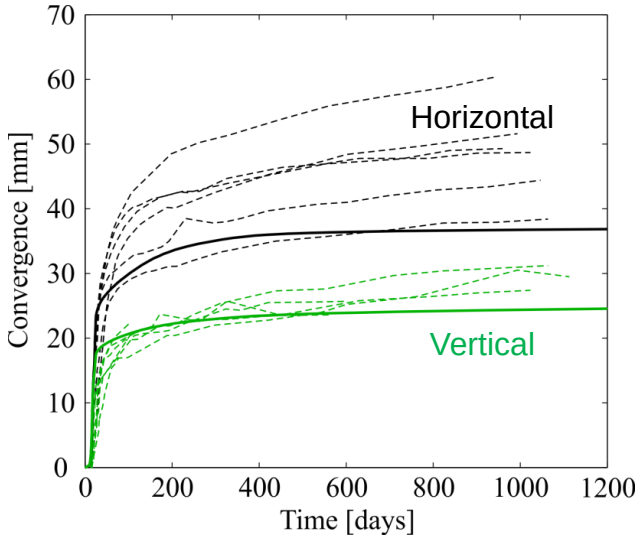

Mine-by experiment

- Displacements

Viscosity based on **in situ measurements** → Viscosity influence

Horizontal

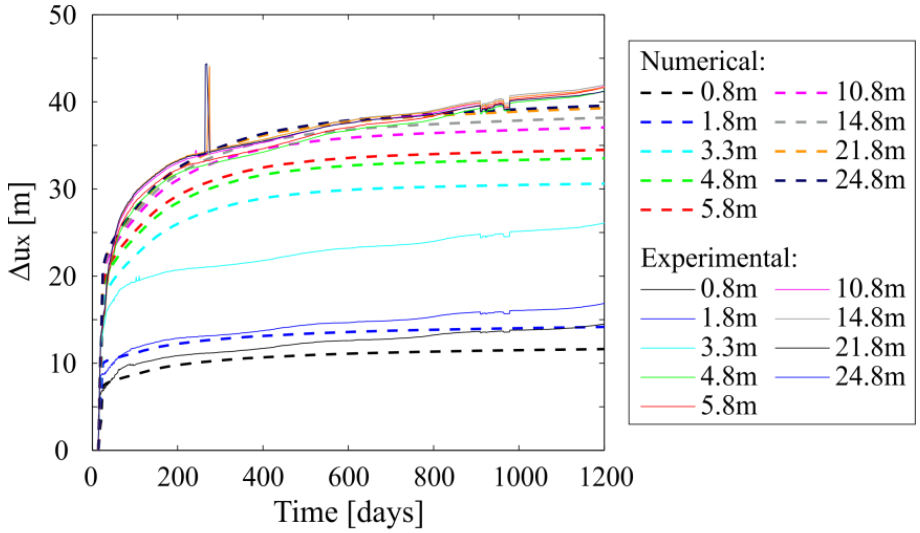

Vertical

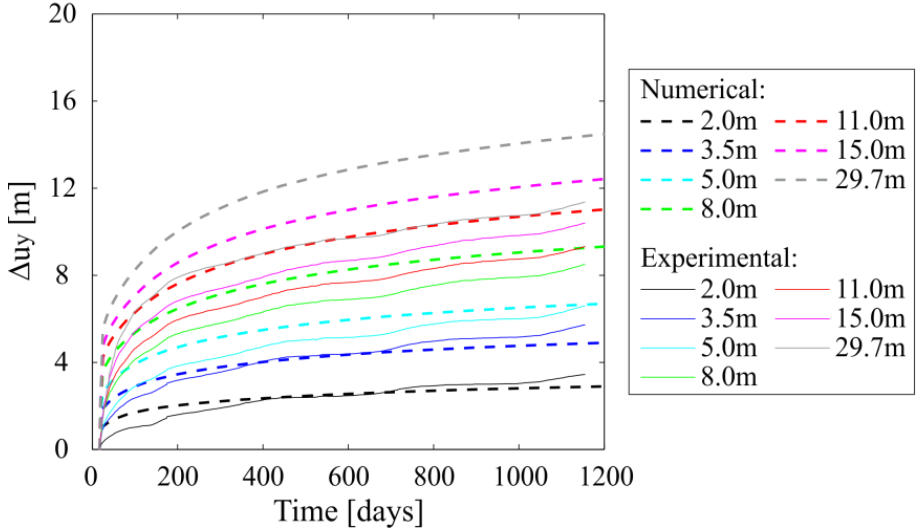

- Convergence

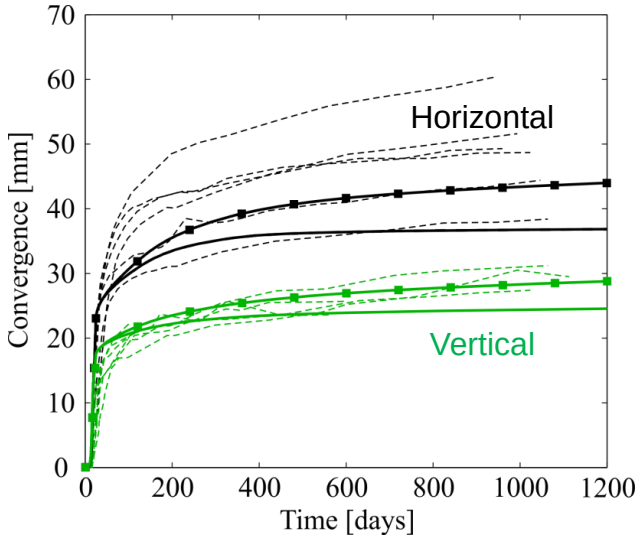

Viscosity allows to reproduce the increase of convergence in the long term.

Mine-by experiment

- Pore water pressure

Mine-by test

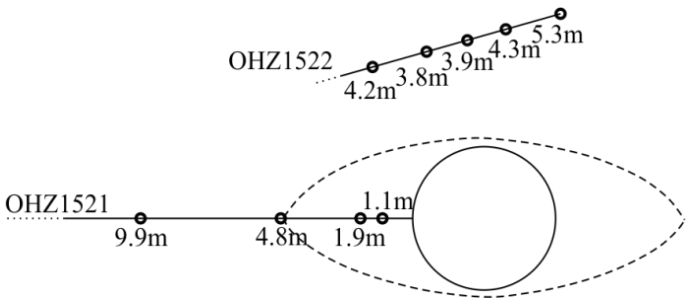

After excavation: RH=100% , p_w = 0 MPa in the gallery

Horizontal: